



Building social resilience in North Korea can mitigate the impacts of climate change on food security

Yu Shi ^{1,2} ^{1,2} ^{1,2} ^{1,2} Ajie Zhang¹, Bingyan Wu¹,², Bin Wang ³, Linchao Li¹,², Hao Shi⁴, Ning Jin⁵, De Li Liu ³, Ruiqing Miao⁶, Xiaoliang Lu¹, Qingling Gengժ, Chaoqun Lu ³, Liang He⁶, Nufang Fang¹, Chao Yue¹, Jianqiang He¹, Hao Feng¹, Shufen Pan⁴, Hanqin Tian ¹¹ and Qiang Yu ¹¹ ^{1,11} ^{1,11}

Adaptation based on social resilience is proposed as an effective measure to mitigate hunger and avoid food shocks caused by climate change. But these have not been investigated comprehensively in climate-sensitive regions. North Korea (NK) and its neighbours, South Korea and China, represent three economic levels that provide us with examples for examining climatic risk and quantifying the contribution of social resilience to rice production. Here our data-driven estimates show that climatic factors determined rice biomass changes in NK from 2000 to 2017, and climate extremes triggered reductions in production in 2000 and 2007. If no action is taken, NK will face a higher climatic risk (with continuous high-temperature heatwaves and precipitation extremes) by the 2080s under a high-emissions scenario, when rice biomass and production are expected to decrease by 20.2% and 14.4%, respectively, thereby potentially increasing hunger in NK. Social resilience (agricultural inputs and population development for South Korea; resource use for China) mitigated climate shocks in the past 20 years (2000–2019), even transforming adverse effects into benefits. However, this effect was not significant in NK. Moreover, the contribution of social resilience to food production in the undeveloped region (15.2%) was far below the contribution observed in the developed and developing regions (83.0% and 86.1%, respectively). These findings highlight the importance of social resilience to mitigate the adverse effects of climate change on food security and human hunger and provide necessary quantitative information.

daptive ability that depends on social–economic resilience is consistently regarded as a crucial factor in coping with climatic risk and safeguarding food security. Social–economic resilience includes not only traditional financial assets and infrastructure¹ but also demographic structure, resource utilization, technology, education, and attitudes and perceptions of risk to change adaptive behaviours².³. However, few studies have integrated social resilience into the climate risk framework to quantify the contribution to regional food production of inherently hard-to-quantify human behaviour and risk perception. Moreover, little is known about the potential of social–economic resilience to mitigate the adverse effects of climate change and extreme events to ensure food security.

North Korea (NK), located in a climate-vulnerable region of eastern Asia (Fig. 1), has been strongly affected by climate change. Many meteorological disasters have induced more severe famine over the past few decades, including typhoons, heavy precipitation events and river floods⁴. According to reports, NK suffered from a freezing disaster in 1993, hail in 1994, severe floods from 1995 to 1996, a typhoon and drought in 1997, and frost in 1998, among other disasters⁵. Even in the twenty-first century, NK's grain production still cannot meet the population's needs, and food deficits still loom large and are even a growing trend^{6,7}.

The similar climatic conditions8 but varying levels of economic development of NK (an undeveloped region according to the World Bank classification) and its neighbours (South Korea (SK), a developed region; and China, a developing region) provide a natural example for investigating the impacts of climate extremes and their link to social-economic resilience9. The similar climatic conditions8 of these areas also rule out uncertainties in social-economic assessments due to differences in climate vulnerability. Comparing economic vulnerability based on social resilience among the three regions with natural adjustment for climate risk is a valuable approach—that is, the ability to adapt to climate risk for food security resulting from climate and economic vulnerability^{10,11}. Here we study rice (Oryza sativa L.), as it is one of the most essential foods in NK. Rice composes more than 60% of the total grain production and directly affects food security for NK in terms of planting area and production¹². Notably, the adverse impacts of climate change on rice systems are increasing13.

Obtaining reliable statistics and survey data from NK is difficult due to NK's politics and economics. Therefore, this study attempted to fully use remote sensing and climate data with openly available statistical information to examine and assess climatic risk and food security with the interaction between climate and

¹State Key Laboratory of Soil Erosion and Dryland Farming on the Loess Plateau, Institute of Soil and Water Conservation, Northwest A&F University, Yangling, China. ²College of Natural Resources and Environment, Northwest A&F University, Yangling, China. ³New South Wales Department of Primary Industries, Wagga Wagga Agricultural Institute, Wagga Wagga, New South Wales, Australia. ⁴International Center for Climate and Global Change Research, College of Forestry, Wildlife and Environment, Auburn University, Auburn, AL, USA. ⁵Department of Resources and Environment, Shanxi Institute of Energy, Jinzhong, China. ⁶Department of Agricultural Economics and Rural Sociology, Auburn University, Auburn, AL, USA. ⁷College of Earth Science and Technology, Zhengzhou University, Zhengzhou, China. ⁸Department of Ecology, Evolution, and Organismal Biology, Iowa State University, Ames, IA, USA. ⁹National Meteorological Center, Beijing, China. ¹⁰Schiller Institute for Integrated Science and Society, Department of Earth and Environmental Sciences, Boston College, Chestnut Hill, MA, USA. ¹¹Key Laboratory of Water Cycle and Related Land Surface Processes, Institute of Geographic Sciences and Natural Resources Research, Chinese Academy of Sciences, Beijing, China. ⁵⁸e-mail: shiyu174274@163.com; tianhan@auburn.edu; yuq@nwafu.edu.cn

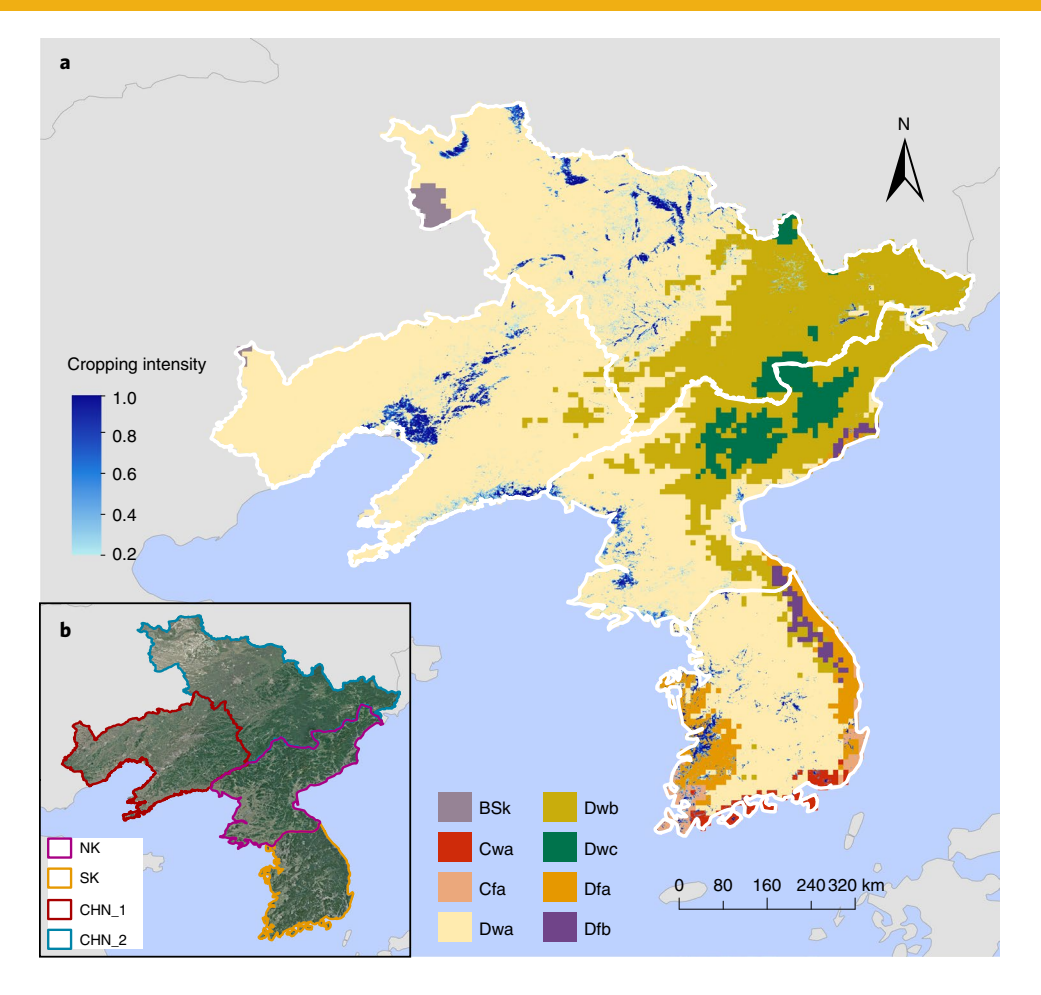


Fig. 1 | Spatial patterns of geographical and climatic distribution across NK, SK, and Liaoning and Jilin provinces of China. a, Climate zones and rice planting intensity from 2000 to 2017. Cropping intensity values of 0.2–0.4 are considered low-frequency rice planting areas, 0.4–0.6 are medium-frequency areas, 0.6–0.8 are high-frequency areas and greater than 0.8 are perennial planting areas. **b**, Geographic boundaries from Google Earth images. BSk, arid and cold steppe; Cwa, temperate regions with dry winter and hot summer; Cfa, temperate regions with hot summer and without dry season; Dwa, cold regions with dry winter and hot summer; Dwb, cold regions with dry winter and warm summer; Dwc, cold regions with dry winter and cold summer; Dfa, cold regions with hot summer and without dry season; Dfb, cold regions with warm summer and without dry season. CHN_1, Liaoning Province of China; CHN_2, Jilin Province of China. The World Bank defines NK, SK and China as low-, high- and upper-middle-income countries/regions, respectively, on the basis of income levels.

social-economic vulnerability for NK and its neighbours (Supplementary Table 1 and Supplementary Fig. 1). In addition, the method presented in this study can be used in regions of the world that lack official information to evaluate climatic risk and food security status (Supplementary Fig. 1). This research intends to answer three interrelated questions: (1) How has climate change (climate extremes) affected rice production in NK in the past? (2) To what extent would projected climate change affect rice production loss in NK in the future? (3) How have human activities (adaptation based on social-economic resilience) exacerbated or ameliorated food deficits in NK and its neighbours? Specifically, we focus on normal and extreme climate changes in NK over a recent past 18-year period (2000–2017), and we attribute rice biomass changes to climatic factors resulting from high-frequency climate extremes and increased vulnerability. The climate projections presented here are based on 27 global climate models (GCMs). The GCMs are derived from the Coupled Model Intercomparison Project Phase 6 (CMIP6) under two future shared socio-economic pathways (SSPs; SSP245 represents SSP2+RCP4.5, a medium-development pathway; SSP585 represents SSP5+RCP8.5, a high-development pathway). Moreover, we assess regional climate changes and resulting production losses from a climatic risk perspective. Finally, the

effects of social resilience are preliminarily explored on the basis of five factors (population development, resource use, science and education, economic development, and agricultural inputs) to mitigate climate shocks for rice production. Furthermore, the contribution of social resilience to rice production is quantified by contrasting the differences between NK and its neighbours (SK and China). More details on the data used, methods and model robustness checks can be found in the Methods and Supplementary Information.

Results

As the representative of the undeveloped and climate-vulnerable regions, NK depends on rice production to feed approximately 25 million people. Our results show that climatic factors determined rice biomass changes in NK from 2000 to 2017, and high-temperature and precipitation extremes triggered reductions in production in 2000 and 2007. If no action is taken, enhanced climate extremes will cause rice production to decrease by the 2080s, further resulting in hunger in NK. Building adaptation based on social resilience in NK, compared with its neighbours (SK, the developed region; and China, the developing region), can mitigate the impacts of climate change on food security.

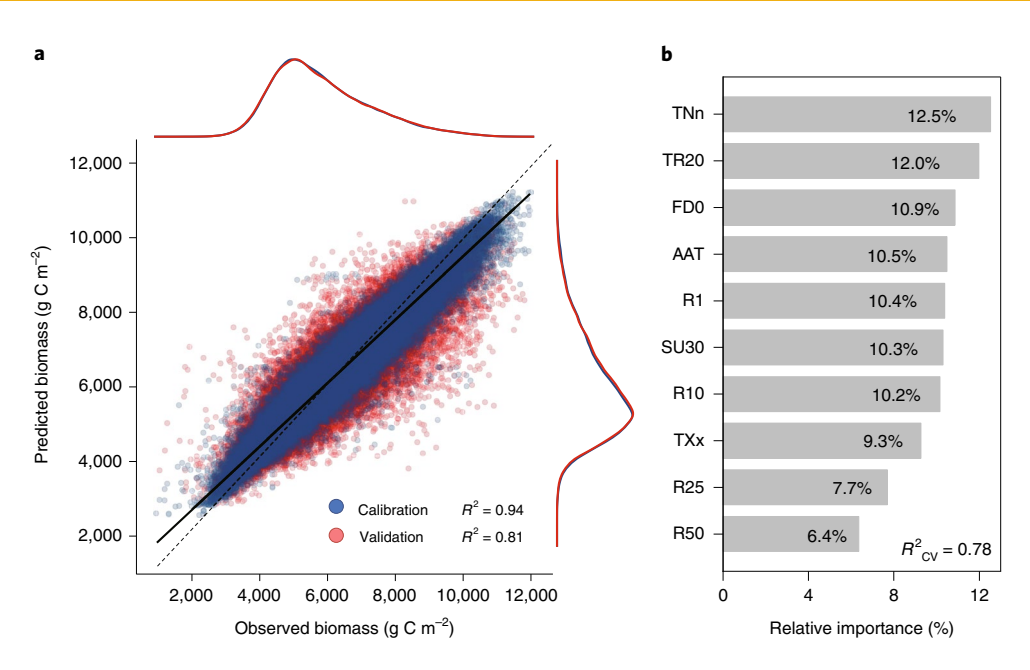


Fig. 2 | Simulating rice biomass and attributing the contribution of climatic variables on the basis of RF modelling in NK. a, Observed versus predicted rice biomass from 2000 to 2017 (baseline period) in NK. The blue and red points represent the calibration and validation datasets, respectively. The dashed and solid black lines are the 1:1 line and the linear trend, respectively. The marginal density in **a** represents the distribution of calibration and validation points in predicted biomass (y axis) and observed biomass (x axis). **b**, Relative importance of climatic variables from RF modelling. See Supplementary Table 3 for the detailed definitions of TS (total solar radiation), AAT, TP, TNn, TXx, TR20, SU30, FD0, R25, R10 (count of days when precipitation was ≥ 10 mm) and R1. R^2_{CV} in **b** represents the goodness of fit from the fivefold cross-validation (Supplementary Table 4).

Domination of climate over the past 18 years for NK. To attribute changes in rice growth and major climate in NK (Fig. 1), the phenology- and pixel-based paddy rice mapping algorithm was first applied on the Google Earth Engine (GEE) cloud platform to extract rice paddy map referencing used by Dong et al. 14 in which they adequately verified this algorithm and the accuracy of rice maps for ensuring robust application in large-scale fields (Supplementary Figs. 2 and 3 and Supplementary Table 2). Furthermore, we adopted an ecosystem light use efficiency (eLUE) model to simulate the biomass of the study areas from 2000 to 2017 and calibrated this model. Supplementary Fig. 4 demonstrates that the eLUE model had good robustness and accurately reproduced the LUE of ecosystems monitored by eddy covariance (EC) towers (tenfold cross-validation: coefficient of determination $(R^2) > 0.75$, normalized root mean squared error (nRMSE) < 0.4, P < 0.01). Consequently, we reestablished the distribution of gross primary productivity (GPP) from 2000 to 2017 using this model for NK (Methods and Supplementary Fig. 1).

The climatic variables that were screened by variance inflation factors (VIFs) were incorporated in the analysis to determine the climate attribution of rice GPP changes in NK over the past 18 years (2000 to 2017) (Supplementary Table 3). More specifically, for NK, climatic variables explained 80% of the GPP changes observed from flux towers from 2000 to 2017 (the baseline period) (Fig. 2a). In addition, temperature (especially temperature extremes) dominated rice GPP changes (explaining nearly 50%) in NK over the expanded period as seen by the four most important variables (TNn, minimum value of the daily minimum temperature; TR20, count of days when the minimum temperature was >20 °C; FD0, count of days when the minimum temperature was <0 °C; and AAT, average air temperature) being related to temperature (Fig. 2b). These results are robust as indicated in the two validation methods (Fig. 2a and Supplementary Table 4). Furthermore, in the 18 years from 2000 to 2017, our results show sudden drops in rice production in 2000 and 2007 (Supplementary Fig. 5). The potential climate shocks induced by climate extremes can cause fluctuations in NK's rice production.

Specifically, extreme heat events and precipitation caused the fluctuations in rice production in 2000 and 2007 (respectively) in NK, as seen by comparing the spatial anomalies of each climatic variable with those in other years. An abnormal increase in extreme heat index was observed in 2000 (TXx, maximum value of the daily maximum temperature in Supplementary Fig. 6), and long-term high temperatures triggered a heatwave that resulted in warming for daytime and overnight periods (TR20 and SU30, count of days when the maximum temperature was >30 °C, in Supplementary Fig. 6). The frequency of abnormal increases in TXx, TR20, SU30 and FD0 in 2000 accounted for 27%, 35%, 37% and 54%, respectively, of the entire region, especially in the western and southern rice-growing areas (Supplementary Figs. 6 and 7). Substantial increases in rain and rainy days were observed in the non-rice part of northeast NK. This did not alleviate the reduction in production caused by the high temperatures and the heatwave (Supplementary Fig. 6). In 2007, precipitation extremes dominated, decreasing rice production in the west/southwest rice-growing region (TP, total precipitation, and R50, count of days when precipitation was ≥ 50 mm, in Supplementary Fig. 6). Specifically, the abnormal increases in TP, R50 and R25 (count of days when precipitation was ≥25 mm) accounted for 87%, 72% and 80%, respectively, of the entire region (Supplementary Fig. 7). Furthermore, the long-term and substantial precipitation produced conditions that made plants highly susceptible to crop root rot and flood damage. These precipitation extremes regulated the surface temperatures, causing the maximum temperatures to decrease and the minimum temperatures to increase (TXx and TNn in Supplementary Fig. 6). Additionally, extreme heat in 2000 and precipitation extremes in 2007 occurred during key phenological stages of rice development—that is, heading-tillering stages that are usually sensitive to climate change and especially sensitive to high temperatures that can cause plant death (Supplementary Fig. 6). In short, rice production in NK decreased abruptly due to extreme weather events (temporally and spatially), resulting in human hunger.

Future climate change and production losses in NK. Here we show the effects of climate change on rice production losses under two climate scenarios (SSP245 and SSP585) based on an ensemble of 27 GCMs (Supplementary Table 5). The future climate would show marked increases in temperature and precipitation in the vulnerable climatic region of NK. Specifically, AAT, TNn and TXx would increase by 2.96 ± 0.93 °C, 2.32 ± 0.59 °C and 3.81 ± 1.12 °C, respectively, under the SSP585 scenario in the 2080s (Supplementary Fig. 8a,d,e). Most surprisingly, SU30 would increase by $97.6 \pm 43.77\%$ and 221.94 ± 77.09% under SSP245 and SSP585, respectively, in the 2080s, indicating that the number of high-temperature days would double and triple in the future compared with the 1979-2018 period (Supplementary Fig. 8g). Additionally, TP, R50 and R25 would increase by $19.93 \pm 7.74\%$, $7.57 \pm 12.53\%$ and $13.42 \pm 9.75\%$, respectively, in the 2080s under SSP585, yet R1 (count of days when precipitation was ≥ 1 mm) would decrease by $19.23 \pm 0.86\%$ (Supplementary Fig. 8c,i,j). In general, no matter which climate scenario is considered, the risk of high temperatures and extreme rainfall due to future warming will increase.

Consequently, with extremely high temperatures and altered precipitation in the future, rice biomass in NK would decrease by 18.9% under SSP245 and by 20.2% under SSP585 in the 2080s, compared with the baseline period. Production would drop by 13% under SSP245 and by 14.4% under SSP585 in the 2080s (Fig. 3a). In NK, where vulnerability to climate is exceptionally high and the frequency of extreme weather leads to low production, 20.2% biomass losses may be conservatively estimated, and the fragile food system may collapse, resulting in famine. In the future, the negative impact caused by climate change on biomass will extend across NK and show different decreasing trends among the regions. The most serious failure of rice biomass was found in the southwest and on the east coast (Fig. 3b), which are the breadbasket of NK (Fig. 1). Despite sporadic increases in biomass, the overall biomass loss from central NK to western coastal areas hides these inconsistent estimates from different climate models. Rice biomass losses projected by the 27 GCMs will become more consistent in the 2080s under the SSP585 scenario (lower standard deviation), which means that the breadbasket areas will be the most extreme hotspots in terms of decreased rice production (Supplementary Fig. 9).

Analysis of adaptability in NK, China and SK. Although rice production is generally subject to natural-environmental change from the standpoint of a climatic risk framework, the adaptive capacity at regional or national levels from social resilience is a greater determinant of rice production losses¹⁵. Social resilience is driven by population, economics, technology and culture³. To quantify the contribution of social resilience to rice production, we collected and used economic statistics from the Food and Agriculture Organization (FAO), the World Bank and an agricultural dataset of remote sensing that involved five factors—population development, resource use, science and education, economic development, and agricultural inputs (Table 1 and Supplementary Table 6)—that together constituted social resilience. Supplementary Figs. 10-12 indicate the correlations between a single social-economic variable and rice production. NK showed weaker correlations between each of the variables of social resilience than SK and China (ρ < 0.5 and no vital significance).

When the climate model incorporated social resilience, more significant explanatory power was shown in SK (P<0.05) and China (P<0.01), but this effect was not substantial in NK (Supplementary Table 7). In addition, social resilience controlled more rice production changes for SK and China (P<0.01), improving the contribution by more than 26% and 100%. Social resilience did not provide additional assistance for NK, which meant that climate dominated rice production changes (Supplementary Table 7). Furthermore, social resilience mitigated climate shocks and even converted adverse effects to benefits in SK and China. Specifically, the notably

high temperature and heatwave (TR20, AAT, TXx and SU30) threatened rice production in SK. However, regional nitrogen fertilizer input, rural population and population aged 0–14 years reversed these effects from climate shocks and even promoted higher rice production (Fig. 4). A similar phenomenon was observed in China, where resources for social resilience relieved damage from rainfall extremes. Specifically, the changes in access to electricity mitigated the negative influence caused by rainfall extremes (R25) (Fig. 4). This significant moderating effect was not observed in NK, where all interactions between climate shocks and social resilience did not result in increased production (Fig. 4).

We conducted a more comprehensive analysis on the basis of random forest (RF) regression of economics (RF_e) to assess the differences in the contributions of social resilience to rice production among NK, SK and China. Of the 12 indexes of social resilience, higher education, rural population and population ages 0-14 dominated rice production variations in NK (P<0.05). Patent applications, population ages 0-14, gross domestic product (GDP) per capita and energy use contributed to rice production variations in SK (P < 0.01). The variation in rice production in China was mainly determined by population ages 0-14, rural population, net official development assistance (ODA) received per capita and GDP per capita (P < 0.05) (Fig. 5a). Economic development and population structure in both developed and developing regions played a more critical role than in undeveloped regions, and science and education in the developed area had a greater influence on rice production than other factors (Fig. 5a). The RF_e analysis further illustrated the essential contribution of social resilience to rice production in SK and China (explaining 83.0% and 86.1%, respectively, of interannual rice production variation, P < 0.05), which was much higher than in NK (15.2%, P < 0.05) (Methods and Fig. 5a). Rice production in developed and developing regions is therefore controlled by social-economic factors (Fig. 5a). In addition, the robust results obtained in this study demonstrate the great potential of social resilience to increase crop production and resist the harmful effects of climate shocks and weather extremes on food security.

Rice production in NK exhibited a threshold-like response to all four important variables influencing rice production, including school enrolment, tertiary (Fig. 5b). Rice production declined when school enrolment was higher than -0.6 units, presumably because limited capital was invested in science education and reduced economic investment and labour from family sources in agriculture. The nonlinear response of rice production in China to population development provided coherent evidence (Fig. 5b). Specifically, rice production decreased with the increasing agricultural population and population ages 0-14 in the undeveloped and developing regions (NK and China) (Fig. 5b). The pressures from dietary needs caused by population growth and the uncoordinated structure of the population constrain economic development and production increases in undeveloped regions¹⁶. For instance, the rural areas with relatively higher mechanization contribute to rice production and require lower agricultural populations¹⁷. In contrast, the response of rice production to population ages 0-14 was the opposite in the developed region (SK), which might be explained by differences in the structure of the population among districts. Developed regions need to increase the proportion of adolescents in the population to adjust for serious ageing18 so that an abundant agricultural labour force is available to increase rice production. Energy use produced an increase in rice production for the developing region (China). Yet, the opposite result was observed for the developed region (SK), owing to the capacity to import resources because of sufficient capital¹⁹. Social resilience probably results in various impacts on rice production among NK, China and SK.

The nonlinear response of rice production to agricultural inputs in the three regions is shown in Supplementary Fig. 13. The response curves for nitrogen, phosphorus and irrigation showed

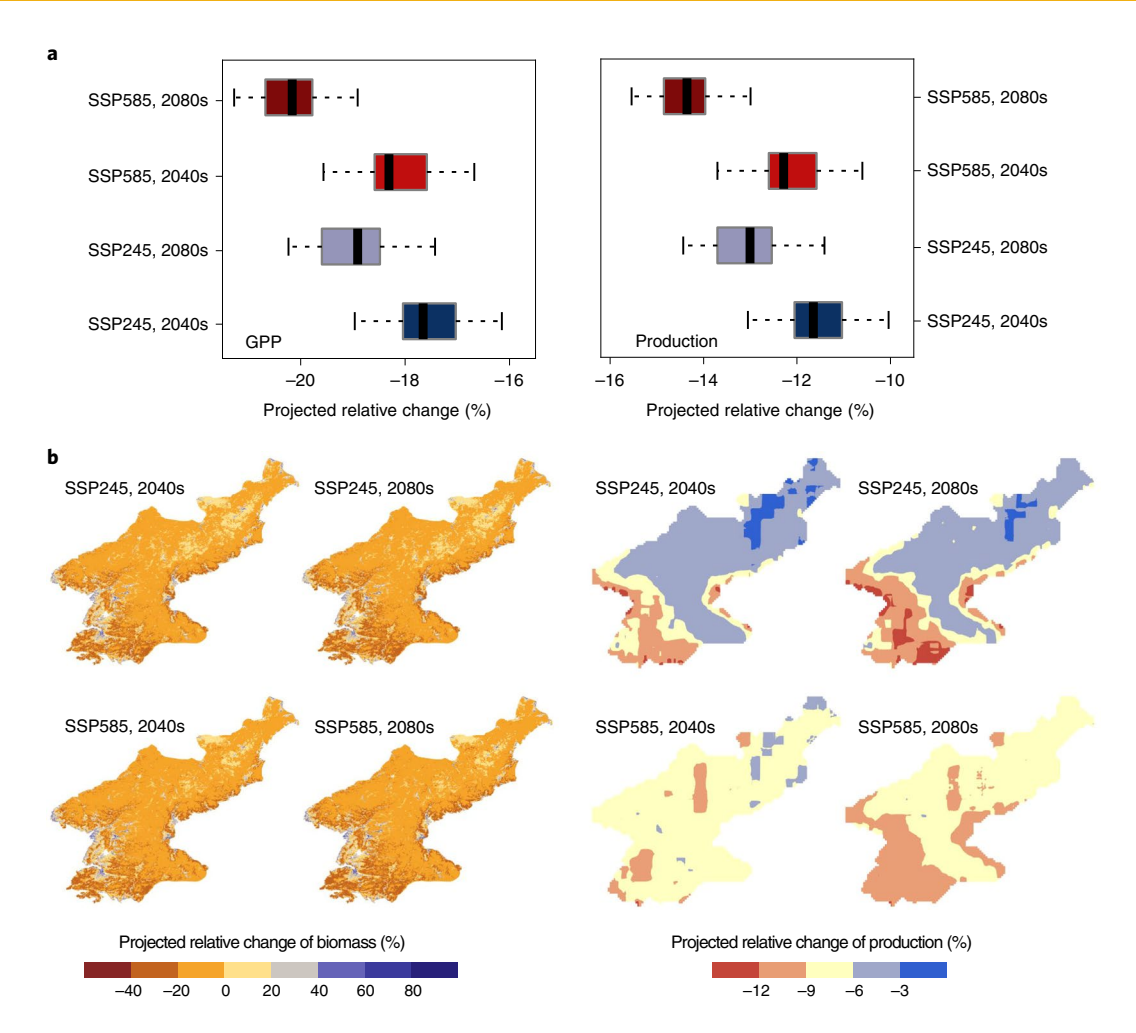


Fig. 3 | Projected rice biomass and production losses under four future scenarios in NK. a,b, The relative change (biomass and production loss) is assessed for the 2040s (2021-2060) and the 2080s (2061-2100) compared with the baseline (2000-2017). SSP245 is SSP2+RCP4.5, an intermediate-development pathway; SSP585 is SSP5+RCP8.5, a high-development pathway. **a**, Box plots of projected rice biomass (left) and production (right) losses under four different future scenarios. The box boundaries indicate the 25th and 75th percentiles across the 27 GCMs, and the whiskers to the left and right of the box edges indicate the 10th and 90th percentiles, respectively. The black line within each box indicates the multi-model median. **b**, Spatial hotspots of rice biomass and production losses under different future scenarios in which biomass changes were measured relative to the baseline period (2000-2017) and production changes were measured relative to production statistics from FAO.

increasing trends in SK and China. However, in NK, the production responses to the three agricultural practice inputs were expressed as humps or concave curves (Supplementary Fig. 13). On the basis of the RF model and its out-of-bag error, agricultural inputs (nitrogen, phosphorus and irrigation) explained -4.8%, 51% and 77% of rice production changes for NK, SK and China, respectively. The explanatory degree for NK was negative, and the three agricultural practices cannot support the increase in rice production in the current situation.

Discussion

Our results demonstrate that climate extremes reduced rice production and that climate warming would contribute to famine in NK. The high-temperature index (SU30) would increase 97.6% and 221.94% under SSP245 and SSP585, respectively, by the 2080s (Supplementary Fig. 8). The number of high-temperature days per year would increase by nearly one month by the 2080s under SSP245, and the number would increase by two months under SSP585. This finding is also supported by results documented in previous literature. Kawasaki and Uchida²⁰ indicated that the abnormal temperature caused by global climate change had a severe negative impact on agricultural production and quality. And climate

extremes will increase in frequency and intensity with rising temperature in the future²¹. Our results also suggest that projected GPP and production may decrease by 20.2% and 14.4% in NK in the 2080s under the SSP585 scenario. However, this result may be underestimated and could be even more severe for crops, because we used the average GPP and harvest index for entire regions to calculate relative changes in biomass. Climate extremes have been known to have critical impacts on the resilience of the food supply chain²². Temperature extremes observed in the past have contributed to increased yield variability, and extreme temperature events will probably increase in the future²³.

However, abnormal weather and climate extremes do not always have negative consequences. Some studies relating to differing weather conditions and intensity and target crops have reported different results in various areas. For instance, Zhao et al.²⁴ indicated that rice yields declined significantly with higher temperature on the basis of simulations of field warming experiments, statistical models and gridded crop models. These yield reductions exceeded assessments by the International Food Policy Research Institute²⁴. Yet, in India, rice yield in the most agro-ecological zones would benefit from climate change predicted by climate scenarios and GCMs²⁵. Furthermore, Lesk et al.²⁶ argued that extreme hourly

Table 1 The vulnerability indexes for social resilience				
Factors of social resilience	Vulnerability indexes	Abbreviation		
Population development (S)	Population ages 0-14 (% of total population)	Pop. 0-14		
	Population ages 15-64 (% of total population)	Pop. 15-64		
	Rural population (% of total population)	RP		
Resource use (H)	Energy use (kg of oil equivalent per capita)	EU		
	Access to electricity (% of population)	AE		
Science and education (S)	School enrolment, tertiary (% gross)	SE		
	Patent applications	PA		
Economic development (H)	Net ODA received per capita (current US\$)	NOR		
	GDP per capita	GDP		
Agricultural inputs	Nitrogen fertilizer use	N		
(H)	Phosphorus fertilizer use	Р		
	Irrigation	Irrigation		
S, soft-adaptive measures; H, hard-adaptive measures.				

rainfall (>50 mm hr⁻¹) caused severe damage to crop yield but that crop growth benefited from heavy rain of 20 mm hr⁻¹. Due to the projected increases in temperature and rainfall intensification in the future, the impact of climate extremes on crops remains somewhat uncertain. It is difficult to identify major changes in climatic sensitivity solely on the basis of production data over time because of the infrequency of extreme weather²⁷. Inductive analysis of the changes in exposure and crop sensitivity to climate extremes is therefore a prerequisite for food security assessment.

Differences in the quantitative attribution in rice production between NK and its neighbours (SK and China) reflected the importance of adaptation based on social resilience to mitigate the adverse effects of extreme climate. Food security may benefit most from changes in adaptive capacity under future climate change, such as agricultural practices, economic development28, resource use and social cognition²⁹. Irrigation³⁰, fertilization, conservation tillage³¹ and crop breeding are being given much attention, with more focus on increasing yields. For example, Challinor et al.32 found that anthropogenic adaptability increases the average yield of crops by 7-15%. However, suppose the focus is only on increasing crop yields. In that case, farmers will still suffer severe production losses due to their low-risk perception concerning the effects of extreme weather disturbances. Learning reflects the ability to produce, absorb and transform new information about climate risk, adaptation and coping with uncertainty. This ability to learn and apply further scientific knowledge is a mitigation mechanism applicable to climate change³³. Capital investment that depends on economic development is a more direct approach. These investments include building early warning systems and climate insurance, resource and energy use, and international trade, as well as reducing poverty. Insurance is a tool to mitigate climatic risk and restore livelihoods, especially in response to climate extremes³⁴. Still, if the insurance structure is not correct, it has an inhibiting effect on risk reduction³⁵. For regions that cannot compensate for losses through trade, these years of low productivity can still be devastating. Undeveloped countries are more vulnerable and less resilient to climate change.

When the poor are struck, they have less support from friends, family and the financial system. Policies meant to reduce poverty under similar climatic risk conditions can also reduce the adverse impacts of climate change^{36,37}. The interaction of social–economic factors from many aspects is the key to decreasing economic vulnerability and increasing social resilience to mitigate climate vulnerability. In this study, social resilience was shown to be enormously important for reducing hunger by contrasting the situation in three regions. Moreover, the topography may limit future rice production potential in NK due to the poor-quality land that is not suitable for planting rice (Supplementary Section 1.1 and Supplementary Fig. 18). Future planning for food security needs to consider climate change and social–economic interactions and development.

This study provides critical insights into the contribution of social resilience to food security. The regions of food insecurity in the world are also the regions with limitations to necessary data due to conflicts, war and climate extremes. A comprehensive evaluation of the food security status in these regions is not only an imperative requirement for sustainable development but also a necessary way to decrease hunger. This study integrated meteorological reanalysis products, openly available statistics and high-resolution imagery to replace unavailable data and ensure robustness. These analyses of food production and food security can therefore be extended to other parts of the globe with ground-truth data limitations. The platform employed in this study, coupled with distinctive regional characteristics, can analyse the importance of social resilience to food security. It has the potential to produce comprehensive assessments of food security status in other regions of the world, such as Africa, Latin America and Southeast Asia. Predictably, national or regional food security is more attributable to social-economic features. Given that food loss occurs from different causes and risks beyond the climate risk framework, global food production is subject to the constraints imposed by exposure and adaptation. For example, food insecurity in most areas of Africa is attributable to an increase in violent conflict since 2014. However, production losses are also attributable to locusts and drought. New insights regarding food security can be obtained for specified regions by incorporating different factors into exposure. This will enable us to further explore the ability of social resilience to mitigate factors that destabilize food security. With the future development of multivariate data (especially remote sensing data), study regions lacking reliable data will have new opportunities for analysis and evaluation.

Our findings are subject to some limitations and should be considered with caution. First, the lack of sufficient ground-truth data for vulnerable regions was the biggest challenge, particularly social economic data (only 20 years). Additionally, we do not resolve other potential sources of uncertainty. For example, the lack of short-term fertilization data and additional management data is a potential source of uncertainty not considered in this study^{38,39}. Second, soil properties may also introduce uncertainty in the results⁴⁰. The physical and chemical properties of soil were different in each region, yet we do not include these in our model. Folberth et al.41 found that assessing the impact of climate change on yield depended on soil type because soil characteristics and moisture buffer or amplify climatic impacts²⁷. This study also did not consider the effects of rice genotype due to a lack of cultivar data, and therefore there may be uncertainty regarding regional production differences⁴². For GPP loss estimation, we did not introduce carbon dioxide (CO2) concentration in our model due to the controversy regarding the ability of increasing CO2 concentration to decrease crop water demand and improve yield while reducing the nutritional content of grain⁴³. Not introducing CO₂ concentration effects may have affected reliable and robust climate and economic vulnerability estimates. Finally, the rice maps and downscaling methods were also sources of uncertainty. Specifically, uncertainties regarding rice maps may have arisen from remote sensing data, poor weather, data quality

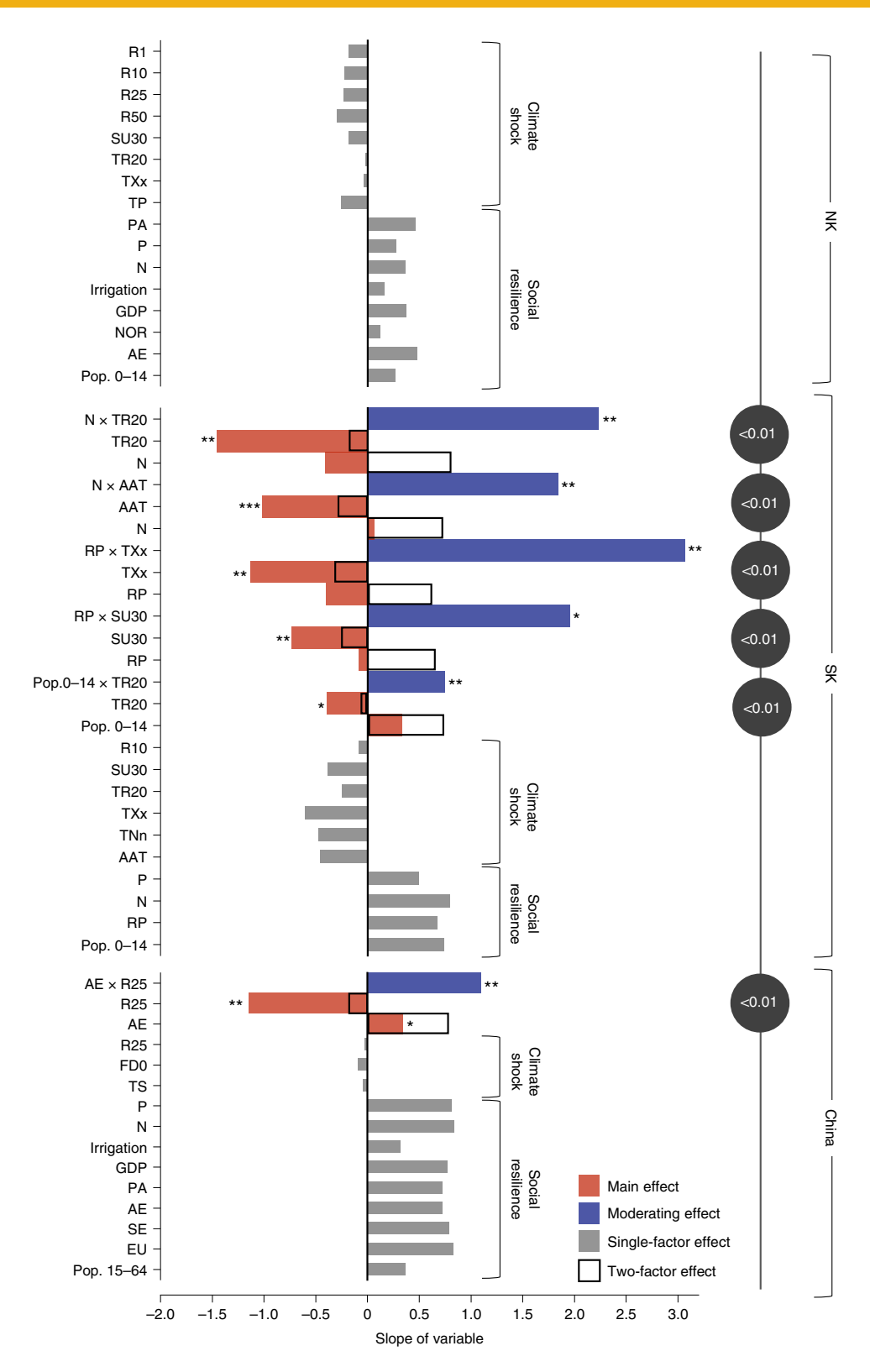


Fig. 4 | Social resilience mitigating climate shocks for rice production in NK, SK and China. All data are normalized to compare positive and negative effects. The slope of each variable (direction and size) represents the positive/negative effect of the specific variable on rice production. The grey bars indicate the slope of the linear regression from social resilience variables (positive) and climate variables (negative). The bars with black borders indicate slopes of the model only containing the independent variable (climate shocks) and the moderator (social resilience). The interactions between social resilience and climate variables are represented as 'A × B' (for example, 'N × TR20'). The red and blue bars represent the slopes of the main effect and the moderating effect, respectively, in each moderation model. The circled values highlight the significance of fit (*P* value) obtained from the *F* statistic for each moderation effect model. * P < 0.0; * **P < 0.00; * **P < 0.01. See Supplementary Table 3 for the detailed definitions of TS, AAT, TP, TNn, TXx, TR20, SU30, FD0, R50, R25, R10 and R1. See Table 1 and Supplementary Table 6 for the detailed definitions of Pop. 15–64, Pop. 0–14, RP, EU, AE, SE, PA, NOR, GDP, N and P.

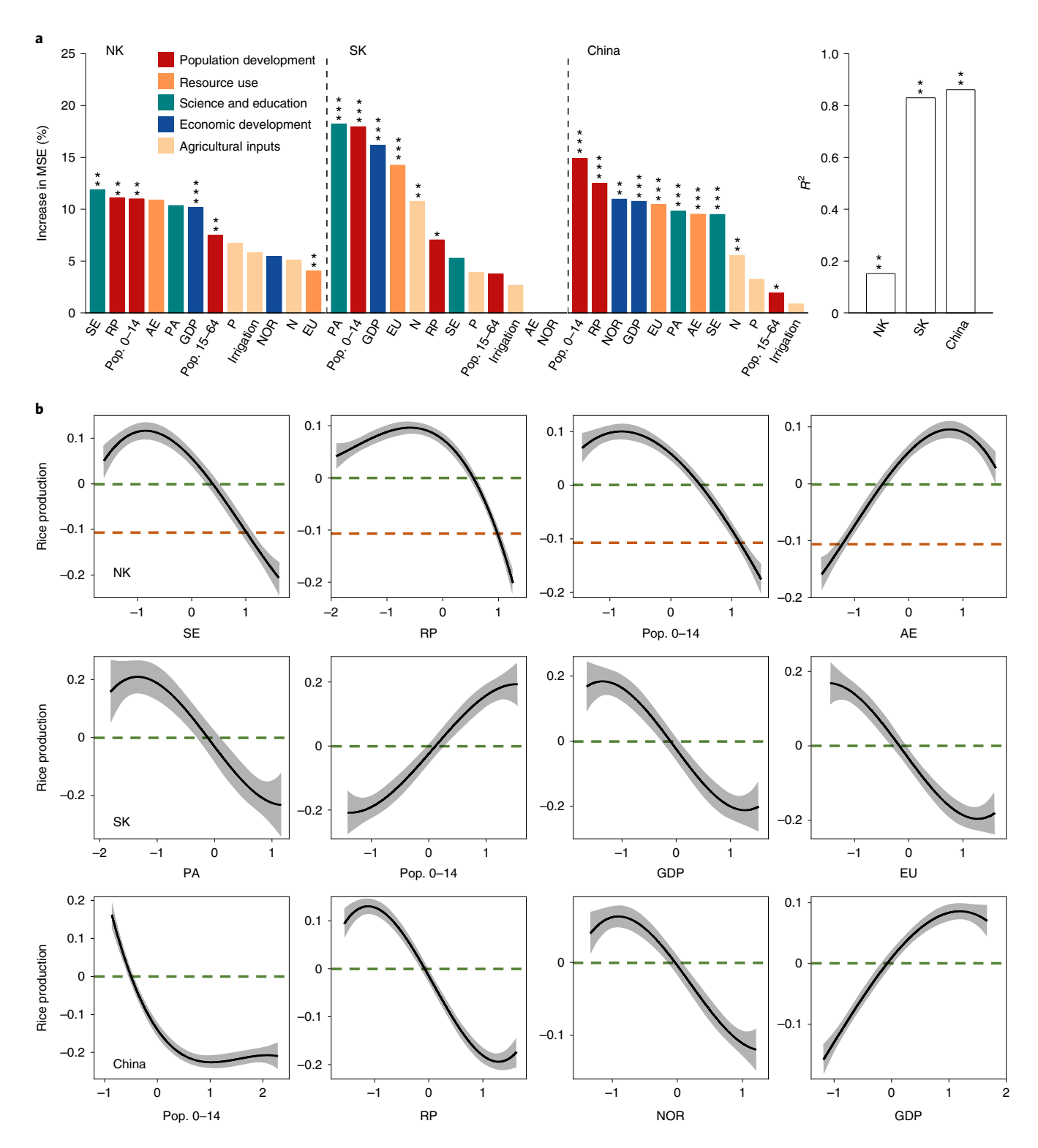


Fig. 5 | The contribution of vulnerability indexes for social resilience to rice production variability. a, The 12 indexes of social resilience are from five factors—that is, population development, resource use, science and education, economic development, and agricultural inputs (Table 1). $^*P < 0.1$; $^{**}P < 0.05$; $^{***}P < 0.01$. *2 indicates the explanation degree of the nonlinear model for contribution of social resilience to rice production in the three regions. MSE, mean squared error. **b**, The nonlinear response of rice production to standardized values of the four most important variables of social resilience. The black lines are smoothed representations of the response using best-fit polynomial equations, with fitted values (model predictions) for the calibration data. The trends of the lines, rather than the actual values, describe the nature of the dependence of rice production on social resilience. The shaded bands denote the 95% confidence intervals. The green and orange dashed lines in the partial dependence plots represent rice production from the baseline and SSP585 scenarios, respectively.

and the number of images observed^{14,44}. This study generated future daily meteorological data with statistical downscaling, but different downscaling methods (such as the change factor method and dynamical downscaling) produced different results⁴⁵. In the future, NK's single-crop production is more likely to lead to food insecurity (rice production accounts for more than 60% of the total food production), leading to hunger. Switching agricultural structures and increasing crop diversity may therefore be a critical path to ensuring food security. The introduction of drought-tolerant and heat-tolerant crops is expected to contribute to food security in vulnerable regions such as NK. Especially at the national level, increasing crop diversity by planting multiple crop species can effectively reduce the losses in national food production, thus ensuring the overall food supply⁴⁶. As one of the crucial components of food system resilience, crop diversity can drive trade diversity, dietary diversity and ecosystem services⁴⁷.

Climate change is expected to increase the frequency and intensity of climate extremes, probably reducing global food production and famines. An accurate assessment of food insecurity must be valued in the deprived areas of the world because it is a vital link in the world food system and is an essential component of the United Nations' Millennium Development Goals. NK is representative of the world's deprived areas, and it and its neighbours offer an excellent example for studying food insecurity in undeveloped regions. Our robust results suggest that social resilience provides a reliable path for understanding and mitigating the detrimental effects of extreme weather shocks in the future. Using this method, we can clarify future food risks and provide quantifiable pathways and goals for efforts. That will contribute to improved national risk awareness, make up for weaknesses in food programmes and guide adjustments to food strategies optimizing social–economic policies.

Methods

Workflow. The workflow presented in this study was designed to assess the contribution of climate change (climate extremes) and social resilience to regional food security. We can use flexible multisource data to extend the study to the rest of the globe, where data availability is restricted (Supplementary Fig. 1). Regional biomass was first simulated on the basis of an eLUE model using observations of flux towers and a remote sensing index (with a 500 m spatial resolution and an eight-day (8d) time step) from NK's neighbours (Liaoning and Jilin provinces of China (CHN_1_2)). We also conducted cross-validation for predicted biomass. Second, we calculated 12 normal and extreme weather variables from ERA-5 reanalysis (with the original 0.1° spatial resolution and a daily step) for NK, SK and CHN_1_2 during the rice growing seasons in 2000 to 2017. These weather variables were used as predictor variables to build a RF model. Furthermore, annual rice distribution was extracted by phenology- and pixel-based paddy rice mapping and satellite products from the Moderate Resolution Imaging Spectroradiometer (MODIS) to mask non-rice regions.

Then, for climate shocks and future climatic risk, two steps were employed. In Step 1, gridded climate variables and biomass in the rice regions from 2000 to 2017 were used as the baseline to build the RF model (RF $_b$). We also validated the stability of the model and calculated the importance of the variables. In Step 2, NK's climatic risk and biomass losses were projected on the basis of the model determined in Step 1 with future climate data that were used for statistical downscaling with daily climate data from ERA-5 (1979 to 2017) and 27 GCMs under SSP245 and SSP585 to assess NK's food security status by the 2040s and the 2080s. Finally, this study included social–economic variables (derived from FAO statistics) and climatic variables (based on daily climatic products of ERA-5) at the national level from 2000 to 2019. The potential for social resilience to mitigate climate shocks in NK, SK and China was explored using a moderation model. We also focused on nonlinear responses of critical variables affecting rice production using an RF $_c$ model and conducted time-series split cross-validation to further clarify the contribution of social resilience to rice production and mitigating climate shocks.

Data sources. We used daily reanalysis data to analyse climate variables over the years of the study. The daily reanalysis data were obtained from the European Center for Medium-Range Weather Forecasts' (ECMWF) gridded dataset at 0.1° resolution. This dataset included daily 2-m temperature (24-hour maximum, minimum and mean temperatures), precipitation and solar radiation from 1979 to 2018. See Supplementary Table 1 for more details. We selected the ECMWF's ERA-5 dataset for two reasons: (1) ground data are not readily available, and (2) by using the global dataset, we can apply our methods to other areas with limited data (Supplementary Table 1).

Our primary analysis calculated three average and nine extreme climate indexes for the 1979–2017 and 2021–2100 periods (Supplementary Table 3). Climatic variables for 2000–2017 were used to attribute extreme weather, modelling regression and prediction for NK. We projected future climatic risk and production losses under different climate scenarios using variables from 2021–2100. We also conducted statistical downscaling of the data from 1979 to 2017 to project future climate change using ERA-5.

We employed the MODIS gridded mosaic for remote sensing information, including 8d surface reflectance, 8d leaf area index and 8d GPP accessed from GEE for 2000–2017 (Supplementary Table 1). We used MODIS surface reflectance to calculate vegetation indexes—that is, normalized difference vegetation index (NDVI), enhanced vegetation index (EVI), land-surface water index (LSWI) and the near-infrared reflectance of vegetation (NIR,). The specific formulas are:

$$EVI = G \frac{\rho_{NIR} - \rho_{Red}}{\rho_{NIR} + C_1 \times \rho_{Red} - C_2 \times \rho_{Blue} + L}$$
 (1)

$$\text{NDVI} = \frac{\rho_{\text{NIR}} - \rho_{\text{Red}}}{\rho_{\text{NIR}} + \rho_{\text{Red}}} \tag{2}$$

$$LSWI = \frac{\rho_{NIR} - \rho_{SWIR}}{\rho_{NIR} + \rho_{SWIR}}$$
 (3)

$$NIR_{v} = NDVI \times \rho_{NIR}$$
 (4)

where $\rho_{\rm Red}$ $\rho_{\rm NIR}$, $\rho_{\rm SWIR}$ and $\rho_{\rm Blue}$ are the surface reflectance values of the red band, the near-infrared band, the shortwave-infrared band and the blue band in the MODIS imagery; L is the canopy background adjustment that addresses nonlinear, differential near-infrared and red radiant transfer through a canopy; C_1 and C_2 are the coefficients of the aerosol resistance term, which uses the blue band to correct for aerosol influences in the red band⁴⁸. And G represents the gain factor. The parameters in the EVI formula are, L=1, $C_1=6$, $C_2=7.5$, and G=2.5.

For geographic information, we also used the digital elevation model with 90-m spatial resolution from SRTM Digital Elevation Data Version 4 in the GEE platform to calculate the slope for every grid cell. All datasets supporting the results of this paper are freely available in Supplementary Table 1.

We accessed the observations of daily net ecosystem CO_2 exchange and ecosystem respiration from two EC towers in the Chinese FLUX Observation and Research Network from 2003–2010 to calibrate and simulate the biomass of the study areas without meteorological inputs (except solar radiation). The EC towers were located close to NK in Yucheng, Shandong province of China (116° 34′ 12.72″ E, 36° 49′ 44.4″ N) and at Changbai Mountain, Jilin province of China (128° 5′ 45″ E, 42° 24′ 9″ N), with farmland and forest ecosystems, respectively. We used the daily net ecosystem exchange and heterotrophic respiration from the flux towers to calculate the gross ecosystem CO_2 exchange. We refer to gross ecosystem CO_2 exchange as gross ecosystem primary productivity (Supplementary Table 1).

The phenological periods of the main crops were obtained from the China Meteorological Data Sharing Service System (http://cdc.cma.gov.cn/home.do) in Panjin Plain, Liaoning province of China, to determine the rice growing and transplanting seasons in the study areas (Supplementary Table 1). We redrew the crop calendar on the basis of Supplementary Table 8 of Zhou et al. 44. The reason for choosing these sites was based on the similar climate zones in the study areas (Fig. 1) and the lack of actual data from NK. All data were strictly examined to meet the standards for further analysis, including cross-validation and comparison with existing data.

The statistical data were obtained from FAO (rice production and population), the United Nations Statistics Division (GDP and imports/exports of goods and services) and the World Bank (population ages 0-14, population ages 15-64, rural population, energy use, access to electricity, school enrolment, patent applications and net ODA received per capita) (Table 1 and Supplementary Table 6). All data are based on the period 2000-2019 at the country level. Nitrogen and phosphorus fertilizer applications for agriculture production were provided by Lu and Tian49, who developed the global gridded data at 0.5° × 0.5° resolution from 1961 to 2013 and published for free access. The statistical data were used to analyse the social-economic attributions. FAO's data quality is generally divided into ten categories: 'Unofficial figure', 'Symbol for indigenous or liveweight meat', 'Official data', 'Aggregate (may include official; semi-official; estimated or calculated data)', 'Calculated', 'FAO estimate', 'Calculated data', 'FAO data based on imputation methodology', 'Data not available' and 'Trend'. More than 95% of the data used in this study were from the 'Official data' and 'Aggregate' categories to ensure high quality.

For further analysis of non-climate attributions, we considered the effect of irrigation on rice growth. We used the water consumption coefficient for rice paddies to replace irrigation because of the lack of irrigation data over the study areas and the large uncertainty in irrigation timing, amounts and methods. The irrigation period for these maps was from 2001 to 2017, and we calculated the ratio of evapotranspiration (from MOD16A2, Supplementary Table 1) to precipitation

as the water consumption coefficient. Furthermore, we averaged the water consumption coefficient for rice paddies in the study areas.

Rice paddy mapping and estimating biomass. Annual rice maps were used to mask non-rice regions to improve the accuracy of the regression model. The annual gridded rice paddy maps (from 2000 to 2017) were produced on the GEE cloud platform on the basis of vegetation indexes (equations (1)–(3)) from MODIS reflectance bands and the calculated rice phenological calendar (Supplementary Table 8 and Supplementary Figs. 2 and 3). See Dong et al. ¹⁴ for clear steps and complete verification. We used very high-resolution samples from Google Earth images to validate the 2015 rice map and obtain high-accuracy rice distributions over NK, SK and CHN_1_2 (Supplementary Table 2 and Supplementary Fig. 3).

Existing biomass products are usually calculated using meteorological data. However, a misleading result can be obtained when analysing which climate variables dominate biomass changes using these products—that is, the climate variables that dominate biomass changes are highly correlated with the climate factors used for the calculation. We therefore considered using a vegetation index from MODIS (with a 500 m spatial resolution and an 8d step) with daily EC tower observations from NK's neighbours (CHN_1_2) to estimate 8d GPP without extra climatic factors (such as temperature and precipitation) for NK. Traditional LUE models need to assess the fraction of absorbed photosynthetically active radiation (fAPAR) and actual LUE (ϵ) separately when calculating GPP. Furthermore, using VIs×PAR_{TOC} to evaluate GPP means that vegetation indexes (VIs) can be more clearly used as a measure of eLUE (described as LUE based on photosynthetically active radiation (PAR))⁵⁰, eLUE is defined as the ratio between GPP and PAR at top-of-canopy (PAR_{TOC}):

$$eLUE_{TOC} = \frac{GPP}{PAR_{TOC}} = f(VIs)$$
 (5)

We averaged daily GPP (GPP $_{\rm EC}$ g C m $^{-2}$ d $^{-1}$) and daily PAR $_{\rm TOC}$ (MJ m $^{-2}$ d $^{-1}$) from two EC towers as 8d values to calculate eLUE $_{\rm TOC}$ (g C MJ $^{-1}$). f(VIs) was from the regression of eLUE $_{\rm TOC}$ to VIs. Once eLUE $_{\rm TOC}$ was estimated, the eLUE relationship with PAR $_{\rm TOC}$ (equation (5)) was rearranged to predict GPP:

$$GPP = eLUE_{TOC} \times PAR_{TOC}$$
 (6)

f(VIs) is the coupling relationship between eLUE and VIs. Past research has focused on the linear model^{50,51}. However, multiple variables have nonlinear relationships in the natural environment, and large-scale areas contain multiple complex ecosystems. The performance of the linear model can no longer meet the practical application in large-scale regions or be extended to other districts. We converted f(VIs) into a nonlinear model (that is, an RF model) and incorporated a variety of VIs into the model (NDVI, EVI, leaf area index and NIRv). RF models have good performance and fewer parameters than other nonlinear models. In recent years, RF models have been widely used in different regions to solve natural science problems at the global scale⁵². For a more detailed explanation of RF models, see Breiman⁵³.

To establish the relationship between eLUE and VIs (calibrating the eLUE model) and provide independent verification, we randomized EC tower data (397 samples) and then divided the data into two subsets for calibration and validation datasets. To evaluate nonlinear model performance, we used a stratified tenfold cross-validation. We used $R^2_{\rm CV}$ and nRMSE $_{\rm CV}$ to evaluate the results of the cross-validation, where the CV subscript represents the data obtained from the cross-validation datasets (5.52). We used the Cal subscript to represent the data obtained from the calibration datasets. These parameters were calculated as:

$$R^{2} = \frac{\left[\sum_{i=1}^{n} (x(i) - x_{m}) (y(i) - y_{m})\right]^{2}}{\sum_{i=1}^{n} (x(i) - x_{m})^{2} \sum_{i=1}^{n} (y(i) - y_{m})^{2}}$$
(7)

$$MSE = \frac{\sum_{i=1}^{n} (pe_i - p_i)^2}{n}$$
 (8)

RMSE =
$$\sqrt{\frac{\sum_{i=1}^{n} (pe_i - p_i)^2}{n}}$$
 (9)

$$nRMSE = \frac{RMSE}{\overline{pe_i}}$$
 (10)

where y(i) and x(i) are the simulated and observed values, respectively; $y_{\rm m}$ and $x_{\rm m}$ represent the mean value, respectively, from simulated and observed series; n is the number of samples; pe_i and p_i are the observed and simulated values, respectively; and $\overline{pe_i}$ is the mean value of the observations.

Attributing predominant climate variables in NK. We downscaled 12 climatic variables (originally 0.1°) to $500\,\mathrm{m}$ resolution and calculated biomass with $500\,\mathrm{m}$ resolution for regional GPP from 2000 to 2017 over NK (see Supplementary

Table 2 for details on the climatic variables). The climatic variables and biomass were then incorporated into an RF model to determine the predominant climate variables. Specifically, all gridded climatic variables with a resolution of 0.1° pixels were resampled to 500 m resolution using the bilinear interpolation method to match biomass. This study's complex models and calculations utilized a large amount of gridded data, resulting in a heavy computation burden and longer times. Hence, we removed the climatic variables whose VIF was greater than 10 to check the multi-collinearity and reduce the computational load and interference in the attribution analysis. The VIF formula was:

$$VIF = \frac{1}{1 - R_i^2} \tag{11}$$

where R^2 represents the coefficient of determination between the *i*th independent variable and other independent variables. Therefore, the variables for solar radiation and rain were excluded from the RF, model.

Compared with linear regression, the nonlinear model explained the nonlinear responses of the climate variables and unravelled the influence of related variables. The process used rice maps to mask non-rice areas. The RF model generated different regression trees using random multiple training sets and features, and each regression tree was sampled independently and distributed identically53. Each regression tree produced different results through branching, and the prediction from the RF regression model was the average of all trees⁵³. The unbiased estimate of RF performance was from out-of-bag (OOB) error, and this result was similar to k-fold cross-validation. For more details about the RF model, please see Breiman⁵³ and Shi et al.⁵². Specifically, RF_b models (Supplementary Table 9) were used to determine the fit between biomass and climatic variables with the parameters 'mtry, the square root of the variables; ntree, 500' in the R program (version 4.0.2; available at https://www.r-project.org) randomForest package (version 4.6-14; available at https://cran.r-project.org/web/packages/randomForest). We further used function importance to compute the variable contribution. The implication of 'importance' is that the permutation of a variable changes the degree of model accuracy—that is, the error rate calculated from samples that did not participate in the training, usually called OOB error. In this study, an increase in MSE percentage was adopted to measure the importance of a variable. Specifically, a variable is permuted, but other variables of OOB samples are kept constant. The RF model is then rerun to obtain new permuted results from OOB. The importance of variables is the average difference between the permuted OOB samples and the original OOB54. Mathematically, the importance of explanatory variables is defined as:

$$VI_X = \frac{1}{N_{\text{tree}}} \sum_{i=1}^{N} (y_{1,i} - y_{2,i})$$
 (12)

where $y_{2,i}$ is calculated from the original OOB samples of RE, $y_{1,i}$ is calculated from the permuted OOB samples and N_{tree} is the number of trees of the RF model. Commonly, larger VI indicates that the explanatory variables are more important.

For NK, SK and CHN_1_2, the percentage of variance explained was calculated by OOB of the RF model as a goodness of fit to assess the response of the climatic variables to biomass (equation (13))²⁵. We validated the stability and accuracy of models on the basis of fivefold cross-validation (Supplementary Section 1.2):

$$1 - \frac{\text{MSE}_{\text{OOB}}}{\delta_{\nu}^2} \tag{13}$$

where δ_{γ}^2 was computed with n as the divisor (rather than n-1). MSE_{OOB} is the mean of squared residuals, calculated as:

$$MSE_{OOB} = \frac{1}{N_{tree}} \sum_{i}^{N} \left(y_i - \hat{y}_i^{OOB} \right)^2$$
 (14)

where \hat{y}_i^{OOB} is the average of the OOB predictions for the ith observation.

We calculated the bias between a specific year and other years during 2000 to 2017 in NK. The ratio of the difference between climatic variables from a specific year and the mean value from other years to the standard deviation of the climatic variables of other years was used to determine the climate anomaly for a specific year. If the anomaly was >1 or <-1, we considered that the values were clearly greater than or less than the others. Specifically, we used the threshold of one standard deviation by assuming that the variations of climatic factors under normal conditions were generally located in the range of one standard deviation about the multi-year mean.

Projections of future climate and biomass losses. We used daily maximum and minimum temperatures, precipitation, and solar radiation from 1979 to 2017 with statistical downscaling and 27 GCMs to calculate climatic variables for different climate scenarios in the future (2021 to 2100), and further calculated three average and nine extreme variables (Supplementary Table 3). The RF_b (Supplementary Table 9) was then used to project annual rice losses under future climate change conditions for spatial pixels over NK from 2000 to 2017. Specifically, we used the statistical downscaling model NWAI-WG⁵⁷ to downscale monthly gridded data from GCMs to daily climate data for 1,299 grid points from meteorological

reanalysis over NK. Statistical downscaling consisted of three major components: spatial downscaling, bias correction and temporal downscaling. Spatial downscaling used inverse distance-weighted interpolation based on the centre of the nearest four grid points in GCMs to improve accuracy⁵⁷, and we then applied bias correction to generate bias-corrected monthly data using a relationship between the observations and GCM data for a historical training period (in this case, 1979–2018). Finally, the daily time series for maximum and minimum temperatures, precipitation, and solar radiation for each pixel were downscaled from the bias-corrected monthly GCM projections using a modified version of the stochastic weather generator⁵⁸. For a more detailed description of statistical downscaling, please see Liu and Zuo⁵⁷.

We downscaled 27 GCMs of CMIP6 (Supplementary Table 5) using the statistical downscaling method as two future climate scenarios (SSP245 and SSP585). Furthermore, the daily average and extreme climate variables were calculated for two climate scenarios from 2021 to 2100 according to the climatic index described above in Supplementary Table 3.

We ran the RF_b model on the basis of gridded climate variables and biomass over NK to project future annual biomass and production losses. Before this, multi-collinearity analysis was conducted on the climate variables (equation (11)). More details about the RF model appear in the previous sections. Two validations were used to examine the robustness of the regression model. First, 75% of the random climate and biomass data from 2000 to 2017 were used as training data, and 25% of the data were used as validation data to test the model performance. The R^2 values were used to evaluate the results of validation and calibration (equation (7)). Second, fivefold cross-validation was conducted (Supplementary Section 1.2 and Supplementary Table 4).

We finally assessed climate change and production loss in the future for the 2040s (2021–2060) and the 2080s (2061–2100). Specifically, for climate change in the future, the relative changes of temperature (AAT, TXx and TNn) were calculated by subtracting the means of the historical period (1979–2017) from the future temperature. For biomass, TS, TP, TR20, SU30, FD0, R50, R25, R10 and R1 (see Supplementary Table 3 for the detailed definitions), the relative changes were derived from the ratio of future means to historical means. For production losses in the future, we obtained the inferred mean value of the conversion coefficient (noted as α) from FAO statistical production (production_F) and estimated regional biomass (that is, α as the ratio of biomass to production). The formulas are:

$$P_{\text{sta}} = \sum_{t}^{B} \times \alpha_{i} \times A \tag{15}$$

$$a_{\text{mean}} = \sum_{i=0}^{n} \frac{a_i}{n} \tag{16}$$

where P_{sta} is statistical production from FAO, \sum_{t1}^{B} represents the sum of each gridded biomass (GPP projected by the RF_b model), α_i represents the conversion coefficient for every year, a_{mean} is the average conversion coefficient calculated by α_i for every year (2000 to 2017), n is the number of years and A is the pixel area (500 m × 500 m).

Future production was projected by using the mean conversion coefficient and predicted GPP by the RF_h model:

$$P_{\text{pre}} = \sum_{l2}^{B} \times \alpha_{\text{mean}} \times A \tag{17}$$

where P_{pre} is future production and \sum_{12}^{B} represents the sum of each predicted GPP. Finally, we used future and historical GPP and production to calculate relative changes as the losses.

The contribution of social resilience to rice production. For NK, SK and China, we examined the contribution of social resilience to mitigating climate shocks and rice production based on national-level climate variables (Supplementary Table 3) and social–economic variables (Table 1 and Supplementary Table 6) from 2000 to 2019. In addition, the nonlinear responses of the four crucial variables to rice production, was explored by the partial dependence for NK, SK and China to describe how social resilience affected rice production changes.

The selection of these variables was based on evidence from previous studies demonstrating that social resilience depends on these economic and social characteristics. A vital understanding of resilience is that the system may transition to another state once a threshold is exceeded, and it is difficult to return to the original state. Thus, resilience is generally regarded as the ability to persist or absorb change while maintaining the same structure and function, and it is described as the magnitude of system change that can be absorbed or that will result in disruption. Social resilience is based on the interdependent relationship between human activities and ecosystems. People are generally more adaptive to social change when they have access to various financial, technological and service resources and to assets. Asset-based societies are usually more adaptive to environmental changes than poor societies, and the rich are more resilient than the poor. Education in social resilience is the key to explaining increasing productivity and income, and a large part of the demographic dividend is derived from the education dividend. In addition, changing population structure is a

direct socio-economic challenge for predicting mitigation and adaptation to inevitable climate change, in which ageing and labour force changes are identified as fundamental socio-economic issues. Energy is a fundamental factor in social-economic development and its ability to eradicate poverty. The preamble of the United Nations' Millennium Development Goals recommends "universal access to affordable, reliable and sustainable energy" and recognizes that "social and economic development depends on the sustainable management of the earth's natural resources" (https://sdgs.un.org/goals/goal7). This study further considered necessary management practices for crop production to resist external stress. The relevant variable references are displayed in Supplementary Table 6. The social resilience data were characterized as one of two types to fully reveal the real social situation: soft-adaptive and hard-adaptive '(Table 1).

We interpolated missing statistics from FAO and the World Bank (national level) from 2000 to 2019 on the basis of linear regression due to discontinuous economic data (four social–economic variables: energy use, school enrolment, access to electricity and patent applications). The range and the filed and interpolated results of the missing data are shown in Supplementary Fig. 14. Specifically, discontinuous economic data for NK were interpolated using regression models to estimate the missing values (energy use, school enrolment, access to electricity and patent applications) (Supplementary Fig. 14; the R^2 values are 0.70, 0.99, 0.99 and 0.92, respectively; the P values are all <0.01).

A moderation model was used to explore the effects of social resilience on mitigating climate shocks⁶⁰. First, we averaged all gridded climate variables (Supplementary Table 3) for NK, SK and China (here using the climatic data in CHN_1_2 as the replacement) to obtain the region-scale value and match the socio-economic variables. Second, all variables were normalized to better compare the positive and negative effects of rice production changes. Furthermore, we screened all adverse climate shocks and positive social resilience to rice production changes on the basis of the linear regression model. The screened negative climate shocks (as independent variables) and positive social resilience (as moderators) were used for pairwise combinations to build a potential production moderation model. Finally, we introduced the interaction between independent variables and moderators in the potential models to explore the mitigation effects of social resilience. Specifically, if the relationship (the direction and size of the slope of the regression) between two variables of interest (the dependent, Y, and independent variables, X) depends on a third moderating variable (the moderator, Z), moderation is said to occur. Here we considered the simple moderating model that is, the following relationship—for hypothesis testing:

$$Y = aX + bZ + cXZ + \varepsilon \tag{18}$$

where Y, X, Z and XZ represent the dependent variables (rice production), the independent variables (negative climate shocks), the moderator (positive social resilience) and the moderating terms, respectively; a, b and c are the coefficients of each regression term; and c is error. If coefficient c is significant (P < 0.1), then D represents a significant moderating effect. Analysis of variance was used to examine the significance of different combinations of variables.

Given that the effects of social resilience on rice production, are often nonlinear, RFe was expected to perform well in assessing the nonlinear relationship. This study modelled the relationship between social-economic variables and rice production on the basis of the RF_e model (Supplementary Table 9) and tested significance for a single variable and the full model using the A3 package (reference, version 1.0.0; available at https://cran.r-project.org/web/packages/A3) in R. Details about the RF regression model and its parameters were provided in the previous section. The parameters of nonlinear models (ntree and mtrv) were set as 500 and the number of the square root of the variables, respectively. The increase in MSE percentage and variance explained were further used as indexes to evaluate variable importance and goodness of fit measures for rice production, (see equations (8), (13) and (14) and the previous section). The partial dependence (that is, marginal effect) was constructed to assess the nonlinear response between rice production, and each of the first four variables. This process was accomplished using the partialPlot function of the randomForest package in R. The threefold time-series split cross-validation was applied to examine the robustness of the RF_e model for NK, SK and China (Supplementary Table 10). We divided the training and validation sets along with time series compared with the original cross-validation. The data from 2000 to 2012 were a test of the first fold, and the data from 2013 to 2014 were the validation of the first fold; the data were further expanded at the two-year step.

Reporting summary. Further information on research design is available in the Nature Research Reporting Summary linked to this article.

Data availability

All original MODIS reflectance and other MODIS products that NASA LP DAAC provided at the USGS EROS Center in this study are freely accessible on the GEE platform at https://developers.google.cn/earth-engine/datasets. The observational, Digital Elevation Model and reanalysis data are publicly available from the following sources: the EC data are at http://www.cnern.org.cn/index.jsp, the ERA5 reanalysis is at https://cds.climate.copernicus.eu/cdsapp#!/dataset/sis-agrometeorological-indicators and the Digital Elevation Model data are at

https://srtm.csi.cgiar.org/. The 27 downscaled GCMs of CMIP6 were provided by D.L.L. and H. Zuo⁵⁷, who downscaled them on the basis of the original CMIP6 at https://esgf-node.llnl.gov/projects/cmip6/. The statistical data are freely available from the following sources: data on rice production, rice imports and exports, fertilizer application, and population from FAO are at http://www.fao.org/faostat/en/; data on GDP from the United Nations Statistics Division are at https://unstats.un.org/unsd/snaama/Basic; and data on population ages 0–14, population ages 15–64, rural population, energy use, access to electricity, school enrolment, patent applications and net ODA received per capita from the World Bank are at https://data.worldbank.org/. Source data are provided with this paper.

Code availability

The first and corresponding authors are prepared to respond to reasonable requests for code.

Received: 5 September 2021; Accepted: 13 June 2022; Published online: 21 July 2022

References

- Smit, B. & Wandel, J. Adaptation, adaptive capacity and vulnerability. Glob. Environ. Change 16, 282–292 (2006).
- Clayton, S. et al. Psychological research and global climate change. Nat. Clim. Change 5, 640–646 (2015).
- Hallegatte, S., Przyluski, V. & Vogt-Schilb, A. Building world narratives for climate change impact, adaptation and vulnerability analyses. *Nat. Clim. Change* 1, 151–155 (2011).
- Wang, B., Xiang, B. & Lee, J.-Y. Subtropical high predictability establishes a promising way for monsoon and tropical storm predictions. *Proc. Natl Acad. Sci. USA* 110, 2718–2722 (2013).
- Bhatia, R. & Thorne-Lyman, A. L. Food shortages and nutrition in North Korea. Lancet 360, s27–s28 (2002).
- Crespo Cuaresma, J. et al. What do we know about poverty in North Korea? Palgr. Commun. 6, 40 (2020).
- McCurry, J. No end in sight for North Korea's malnutrition crisis. Lancet 379, 602 (2012).
- Beck, H. E. et al. Present and future Köppen–Geiger climate classification maps at 1-km resolution. Sci. Data 5, 180214 (2018).
- Yun, J. & Jeong, S. Contributions of economic growth, terrestrial sinks, and atmospheric transport to the increasing atmospheric CO₂ concentrations over the Korean Peninsula. *Carbon Balance Manage.* 16, 22 (2021).
- Aerts, J. C. J. H. et al. Integrating human behaviour dynamics into flood disaster risk assessment. Nat. Clim. Change 8, 193–199 (2018).
- Sarkodie, S. A. & Strezov, V. Economic, social and governance adaptation readiness for mitigation of climate change vulnerability: evidence from 192 countries. Sci. Total Environ. 656, 150–164 (2019).
- Gunjal, K. et al. FAO/WFP Crop and Food Security Assessment Mission to the Democratic People's Republic of Korea (Food and Agriculture Organization of the United Nations/World Food Programme, 2013).
- Chen, X. et al. The effects of projected climate change and extreme climate on maize and rice in the Yangtze River Basin, China. Agric. For. Meteorol. 282–283, 107867 (2020).
- Dong, J. et al. Mapping paddy rice planting area in northeastern Asia with Landsat 8 images, phenology-based algorithm and Google Earth Engine. Remote Sens. Environ. 185, 142–154 (2016).
- Barnes, M. L. et al. Social determinants of adaptive and transformative responses to climate change. Nat. Clim. Change 10, 823–828 (2020).
- Schneider, U. A. et al. Impacts of population growth, economic development, and technical change on global food production and consumption. *Agric.* Syst. 104, 204–215 (2011).
- Amare, D. & Endalew, W. Agricultural mechanization: assessment of mechanization impact experiences on the rural population and the implications for Ethiopian smallholders. *Eng. Appl. Sci.* 1, 39–48 (2016).
- Kim, H. K. & Lee, S.-H. The effects of population aging on South Korea's economy: the National Transfer Accounts approach. J. Econ. Ageing 20, 100340 (2021).
- Scheelbeek, P. F. D. et al. United Kingdom's fruit and vegetable supply is increasingly dependent on imports from climate-vulnerable producing countries. *Nat. Food* 1, 705–712 (2020).
- Kawasaki, K. & Uchida, S. Quality matters more than quantity: asymmetric temperature effects on crop yield and quality grade. Am. J. Agric. Econ. 98, 1195–1209 (2016).
- Wang, G. et al. The peak structure and future changes of the relationships between extreme precipitation and temperature. *Nat. Clim. Change* 7, 268–274 (2017).
- Hansen, J., Sato, M. & Ruedy, R. Perception of climate change. Proc. Natl Acad. Sci. USA 109, E2415–E2423 (2012).
- 23. Hawkins, E. et al. Increasing influence of heat stress on French maize yields from the 1960s to the 2030s. *Glob. Change Biol.* **19**, 937–947 (2013).

- Zhao, C. et al. Plausible rice yield losses under future climate warming. Nat. Plants 3, 16202 (2016).
- Gupta, R. & Mishra, A. Climate change induced impact and uncertainty of rice yield of agro-ecological zones of India. Agric. Syst. 173, 1–11 (2019).
- Lesk, C., Coffel, E. & Horton, R. Net benefits to US soy and maize yields from intensifying hourly rainfall. *Nat. Clim. Change* 10, 819–822 (2020).
- Lobell, D. B., Deines, J. M. & Tommaso, S. D. Changes in the drought sensitivity of US maize yields. *Nat. Food* 1, 729–735 (2020).
- Acevedo, M. et al. A scoping review of adoption of climate-resilient crops by small-scale producers in low- and middle-income countries. *Nat. Plants* 6, 1231–1241 (2020).
- Engle, N. L. Adaptive capacity and its assessment. Glob. Environ. Change 21, 647–656 (2011).
- Fang, W. et al. Probabilistic assessment of remote sensing-based terrestrial vegetation vulnerability to drought stress of the Loess Plateau in China. Remote Sens. Environ. 232, 111290 (2019).
- Corbeels, M., Naudin, K., Whitbread, A. M., Kühne, R. & Letourmy, P. Limits of conservation agriculture to overcome low crop yields in sub-Saharan Africa. Nat. Food 1, 447–454 (2020).
- Challinor, A. J. et al. A meta-analysis of crop yield under climate change and adaptation. Nat. Clim. Change 4, 287–291 (2014).
- Neil Adger, W., Arnell, N. W. & Tompkins, E. L. Successful adaptation to climate change across scales. Glob. Environ. Change 15, 77–86 (2005).
- 34. Surminski, S., Bouwer, L. M. & Linnerooth-Bayer, J. How insurance can support climate resilience. *Nat. Clim. Change* **6**, 333–334 (2016).
- Miao, R. Climate, insurance and innovation: the case of drought and innovations in drought-tolerant traits in US agriculture. Eur. Rev. Agric. Econ. 47, 1826–1860 (2020).
- Hsiang, S. et al. Estimating economic damage from climate change in the United States. Science 356, 1362–1369 (2017).
- 37. De Cian, E., Hof, A., Marangoni, G., Tavoni, M. & Van Vuuren, D. Alleviating inequality in climate policy costs: an integrated perspective on mitigation, damage and adaptation. *Environ. Res. Lett.* 11, 074015 (2016).
- Spehar, C. R. Impact of strategic genes in soybean on agricultural development in the Brazilian tropical savannahs. Field Crop. Res. 41, 141–146 (1995).
- Butler, E. E., Mueller, N. D. & Huybers, P. Peculiarly pleasant weather for US maize. Proc. Natl Acad. Sci. USA 115, 11935–11940 (2018).
- Bossio, D. A. et al. The role of soil carbon in natural climate solutions. Nat. Sustain. 3, 391–398 (2020).
- 41. Folberth, C. et al. Uncertainty in soil data can outweigh climate impact signals in global crop yield simulations. *Nat. Commun.* 7, 11872 (2016).
- Wang, X. et al. Breeding rice varieties provides an effective approach to improve productivity and yield sensitivity to climate resources. *Eur. J. Agron.* 124, 126239 (2021).
- Hasegawa, T. et al. Risk of increased food insecurity under stringent global climate change mitigation policy. Nat. Clim. Change 8, 699–703 (2018).
- Zhou, Y. et al. Mapping paddy rice planting area in rice-wetland coexistent areas through analysis of Landsat 8 OLI and MODIS images. *Int. J. Appl. Earth Obs. Geoinf.* 46, 1–12 (2016).
- Wang, B. et al. Sources of uncertainty for wheat yield projections under future climate are site-specific. Nat. Food 1, 720–728 (2020).
- Renard, D. & Tilman, D. National food production stabilized by crop diversity. *Nature* 571, 257–260 (2019).
- 47. Hertel, T., Elouafi, I., Tanticharoen, M. & Ewert, F. Diversification for enhanced food systems resilience. *Nat. Food* 2, 832–834 (2021).
- Huete, A. et al. Overview of the radiometric and biophysical performance of the MODIS vegetation indices. Remote Sens. Environ. 83, 195–213 (2002).
- Lu, C. & Tian, H. Global nitrogen and phosphorus fertilizer use for agriculture production in the past half century: shifted hot spots and nutrient imbalance. Earth Syst. Sci. Data 9, 181–192 (2017).
- Ma, X. et al. Parameterization of an ecosystem light-use-efficiency model for predicting savanna GPP using MODIS EVI. Remote Sens. Environ. 154, 253–271 (2014).
- Ma, X. et al. Spatiotemporal partitioning of savanna plant functional type productivity along NATT. Remote Sens. Environ. 246, 111855 (2020).
- Shi, Y. et al. Attribution of climate and human activities to vegetation change in China using machine learning techniques. Agric. For. Meteorol. 294, 108146 (2020).
- 53. Breiman, L. Random forests. Mach. Learn. 45, 5-32 (2001).
- Liaw, A. & Wiener, M. Classification and regression by randomForest. R News
 18–22 (2002).
- 55. Lewis, S. L., Brando, P. M., Phillips, O. L., van der Heijden, G. M. F. & Nepstad, D. The 2010 Amazon drought. *Science* 331, 554 (2011).
- Wang, S. et al. Warmer spring alleviated the impacts of 2018 European summer heatwave and drought on vegetation photosynthesis. *Agric. For. Meteorol.* 295, 108195 (2020).
- Liu, D. L. & Zuo, H. Statistical downscaling of daily climate variables for climate change impact assessment over New South Wales, Australia. *Climatic Change* 115, 629–666 (2012).

- 58. Richardson, C. & Wright, D. WGEN: A Model for Generating Daily Weather Variables (USDA Agricultural Research Service, 1984).
- Logan, T. M., Guikema, S. D. & Bricker, J. D. Hard-adaptive measures can increase vulnerability to storm surge and tsunami hazards over time. *Nat. Sustain.* 1, 526–530 (2018).
- Hogan, P. S., Chen, S. X., Teh, W. W. & Chib, V. S. Neural mechanisms underlying the effects of physical fatigue on effort-based choice. *Nat. Commun.* 11, 4026 (2020).

Acknowledgements

This study was supported by the collaboration project jointly founded by the NSFC (grant no. 41961124006) and the NSF (grant no. 1903722) for Innovations at the Nexus of Food, Energy, and Water Systems (INFEWS: US–China). H.T. acknowledges funding support from the Andrew Carnegie Fellow Program (award no. G-F-19-56910).

Author contributions

Q.Y. and H.T. designed the study. Y.S. analysed the modelling results, created the figures and wrote the draft of the paper. Y.Z., B. Wu, H.S., L.L. and N.J. provided technology services and analysed the data. L.L. and B. Wang were responsible for technical support and manuscript editing of the partial dependence analysis. D.L.L. provided the

downscaled GCM data of CMIP6. R.M. provided edits and suggestions for the social-economic analysis. X.L., Q.G., C.L., L.H., N.F., C.Y., J.H., H.F. and S.P. contributed to the interpretation of the results and the writing of the manuscript.

Competing interests

The authors declare no competing interests.

Additional information

Supplementary information The online version contains supplementary material available at https://doi.org/10.1038/s43016-022-00551-6.

Correspondence and requests for materials should be addressed to Yu Shi, Hanqin Tian or Qiang Yu.

Peer review information *Nature Food* thanks Matthew Cooper, Sujong Jeong and Tao Lin for their contribution to the peer review of this work.

Reprints and permissions information is available at www.nature.com/reprints.

Publisher's note Springer Nature remains neutral with regard to jurisdictional claims in published maps and institutional affiliations.

© The Author(s), under exclusive licence to Springer Nature Limited 2022

nature portfolio

Corresponding author(s):	Qiang Yu
Last updated by author(s):	May 24, 2022

Reporting Summary

Nature Portfolio wishes to improve the reproducibility of the work that we publish. This form provides structure for consistency and transparency in reporting. For further information on Nature Portfolio policies, see our Editorial Policies and the Editorial Policy Checklist.

<u> </u>			0.00	
St	'a'	۲ı۹	:†1	CS

For	all statistical analyses, confirm that the following items are present in the figure legend, table legend, main text, or Methods section.
n/a	Confirmed
	The exact sample size (n) for each experimental group/condition, given as a discrete number and unit of measurement
	A statement on whether measurements were taken from distinct samples or whether the same sample was measured repeatedly
	The statistical test(s) used AND whether they are one- or two-sided Only common tests should be described solely by name; describe more complex techniques in the Methods section.
\boxtimes	A description of all covariates tested
\boxtimes	A description of any assumptions or corrections, such as tests of normality and adjustment for multiple comparisons
	A full description of the statistical parameters including central tendency (e.g. means) or other basic estimates (e.g. regression coefficient) AND variation (e.g. standard deviation) or associated estimates of uncertainty (e.g. confidence intervals)
	For null hypothesis testing, the test statistic (e.g. <i>F</i> , <i>t</i> , <i>r</i>) with confidence intervals, effect sizes, degrees of freedom and <i>P</i> value noted <i>Give P values as exact values whenever suitable.</i>
\boxtimes	For Bayesian analysis, information on the choice of priors and Markov chain Monte Carlo settings
\boxtimes	For hierarchical and complex designs, identification of the appropriate level for tests and full reporting of outcomes
	Estimates of effect sizes (e.g. Cohen's <i>d</i> , Pearson's <i>r</i>), indicating how they were calculated
	Our web collection on <u>statistics for biologists</u> contains articles on many of the points above.

Software and code

Policy information about availability of computer code

Data collection

No software was used to collect data in this study. All data were from publicly available sources, which were downloaded directly. The sources have been described in the manuscript.

Data analysis

Microsoft Excel (version Professional Plus 2019) was used to prepare and harmonize data. Remote sensing data were obtained and preprocessed from Google Earth Engine. R version 4.0.2 was used by authors for aggregating and analyzing the climate data and modeling results. The spatial distribution maps were plotted in ArcGIS version 10.6, and the rest of the figures were plotted in Origin version 2021 and R version 4.0.2. The codes for data analysis and plot figures were available from the corresponding author upon reasonable request.

For manuscripts utilizing custom algorithms or software that are central to the research but not yet described in published literature, software must be made available to editors and reviewers. We strongly encourage code deposition in a community repository (e.g., GitHub), See the Nature Portfolio guidelines for submitting code & software for further information.

Data

Policy information about <u>availability of data</u>

All manuscripts must include a data availability statement. This statement should provide the following information, where applicable:

- Accession codes, unique identifiers, or web links for publicly available datasets
- A description of any restrictions on data availability
- For clinical datasets or third party data, please ensure that the statement adheres to our policy

All historical data used are publicly available and open access, with the data sources listed in Methods. The other data (regional GPP) that support the findings of this study are available from the corresponding author upon reasonable request. In addition, we list all data sources below:

All original MODIS reflectance and other MODIS products that were provided by NASA LP DAAC at the USGS EROS Center in this study are freely accessible on the GEE platform (https://developers.google.cn/earth- engine/datasets).

The observational, DEM, and reanalysis data are publicly available from the following sources:

- -EC data (http://www.cnern.org.cn/index.jsp)
- -ERA5 reanalysis(https://cds.climate.copernicus.eu/cdsapp#!/dataset/sis-agrometeorological-indicators)
- -DEM data (https://srtm.csi.cgiar.org/)

The downscaled 27 GCMs of CMIP6 were kindly provided by the co-authors of Liu et al. who downscaled them based on the original CMIP6 (https://esgf-node.llnl.gov/projects/cmip6/)

The statistical data are freely available from the following sources:

- -rice production, rice imports and exports, fertilizer application, and population from FAO (http://www.fao.org/faostat/en/)
- -GDP from United Nations Statistics Division (https://unstats.un.org/unsd/snaama/Basic)
- -Population ages 0-14, Population ages 15-64, Rural population, Energy use, Access to electricity, School enrollment, Patent applications, and Net ODA received per capita from World Bank (https://data.worldbank.org/)

Field-specific reporting

ł	Please select the one below	that is the best f	it for your research.	. It yo	u are not sure,	read the	appropriate	sections befor	e making your	selection
Γ	Life sciences	Behavioural	& social sciences	\boxtimes	Ecological, ev	olutionar	y & environm	nental sciences		

For a reference copy of the document with all sections, see <u>nature.com/documents/nr-reporting-summary-flat.pdf</u>

Life sciences study design

All studies must disclose on these points even when the disclosure is negative.

Sample size

Describe how sample size was determined, detailing any statistical methods used to predetermine sample size OR if no sample-size calculation was performed, describe how sample sizes were chosen and provide a rationale for why these sample sizes are sufficient.

Data exclusions

Describe any data exclusions. If no data were excluded from the analyses, state so OR if data were excluded, describe the exclusions and the rationale behind them, indicating whether exclusion criteria were pre-established.

Replication

Describe the measures taken to verify the reproducibility of the experimental findings. If all attempts at replication were successful, confirm this OR if there are any findings that were not replicated or cannot be reproduced, note this and describe why.

Randomization

Describe how samples/organisms/participants were allocated into experimental groups. If allocation was not random, describe how covariates were controlled OR if this is not relevant to your study, explain why.

Blinding

Describe whether the investigators were blinded to group allocation during data collection and/or analysis. If blinding was not possible, describe why OR explain why blinding was not relevant to your study.

Behavioural & social sciences study design

All studies must disclose on these points even when the disclosure is negative.

Study description

Briefly describe the study type including whether data are quantitative, qualitative, or mixed-methods (e.g. qualitative cross-sectional, quantitative experimental, mixed-methods case study).

Research sample

State the research sample (e.g. Harvard university undergraduates, villagers in rural India) and provide relevant demographic information (e.g. age, sex) and indicate whether the sample is representative. Provide a rationale for the study sample chosen. For studies involving existing datasets, please describe the dataset and source.

Sampling strategy

Describe the sampling procedure (e.g. random, snowball, stratified, convenience). Describe the statistical methods that were used to predetermine sample size OR if no sample-size calculation was performed, describe how sample sizes were chosen and provide a rationale for why these sample sizes are sufficient. For qualitative data, please indicate whether data saturation was considered, and what criteria were used to decide that no further sampling was needed.

Data collection

Provide details about the data collection procedure, including the instruments or devices used to record the data (e.g. pen and paper, computer, eye tracker, video or audio equipment) whether anyone was present besides the participant(s) and the researcher, and whether the researcher was blind to experimental condition and/or the study hypothesis during data collection.

Timing

Indicate the start and stop dates of data collection. If there is a gap between collection periods, state the dates for each sample cohort.

Data exclusions

If no data were excluded from the analyses, state so OR if data were excluded, provide the exact number of exclusions and the rationale behind them, indicating whether exclusion criteria were pre-established.

Non-participation

State how many participants dropped out/declined participation and the reason(s) given OR provide response rate OR state that no participants dropped out/declined participation.

Ecological, evolutionary & environmental sciences study design

All studies must disclose on these points even when the disclosure is negative.

Study description

Adaption based on social resilience is proposed as an effective measure to mitigate hunger and avoid disasters caused by climate change. But these have not been investigated comprehensively in climate sensitive regions, especially regarding the necessary quantitative paths. North Korea (NK, undeveloped) and its neighbors (South Korea, developed; China, developing) represent three economic levels that provide us with examples for examining climatic risk and quantifying the contribution of social resilience to rice production. Our data-driven estimates showed that climatic factors determined rice biomass changes in NK, and climate extremes triggered reductions in production. If no action is taken, NK will face a higher climatic risk (with continuous high temperature heatwaves and precipitation extremes) by the 2080s under a high emission scenario when rice biomass and production are expected to decrease by 20.2% and 14.4%, respectively, thereby potentially increasing hunger in NK. Social resilience (agricultural inputs and population development for South Korea; resource use for China) mitigated climate shocks, even transforming adverse effects into benefits. However, this effect was not significant in NK. Moreover, the contribution of social resilience to food production in the undeveloped region (15.2%) was far below the contribution observed in the developed and developing regions (83.0% and 86.1%, respectively). These findings highlight the importance of social resilience to mitigate the adverse effects of climate change on food security and human hunger and provide necessary quantitative information.

Research sample

The observed climate data were used to analyze climatic risk of rice biomass and production during 2000-2017. The GCM data under SSP245 and SSP585 for future years (2021-2100) were split into two parts (2021-2060 and 2061-2100) for rice biomass and production simulations, which was a standard practice in the field of climate change studies. Other datasets including remote sensing index, site observation, crop calendar, DEM, and statistics were collected from various publicly available datasets on environment and society, which was described in the Method section.

Sampling strategy

To include as many samples as possible, all the regional rice observations over North Korea and all the social-economic variables during 2000-2019 were used for the regression. Additionally, to project future biomass losses, the 75% baseline data were randomly sampled as training data sets. The machine learning techniques for building models and analyzing results in this study were tested based on k-fold cross validation, reporting in the supplementary information.

Data collection

Y. Shi collected data from various publicly available datasets on environment and society, and downloaded vegetation index and other MODIS products from Google Earth Engine platform. Liu used a statistical downscaling (SD) method to generate future daily climate data.

Timing and spatial scale

Timing scale: the historical meteorological reanalysis and the future projection ranged over 1979-2018, 2021-2060 and 2061-2100, respectively. The environmental variables for assessing rice biomass were collected during 2000-2017, and social-economic variables were from datasets published during 2000-2019.

Spatial scale: original meteorological reanalysis with 0.5° X 0.5° resolution were downscaled as 500m X 500m resolution to match biomass with similar resolution.

Data exclusions

No data were excluded from the analyses

Reproducibility

All data will be publicly available to reproduce the results. We can provide code and technical help if readers are interested.

Randomization

Our work was based on random forest models simulations, and this model already had excellent randomization. Additionally, to project future biomass losses, the 75% baseline data were randomly sampled as training data sets. The machine learning techniques in this study were tested based on k-fold cross validation for meeting randomization.

Blinding

We used open-historical records, so blinding was not relevant to this study.

Did the study involve field work?

Field work, collection and transport

Field conditions

Describe the study conditions for field work, providing relevant parameters (e.g. temperature, rainfall).

Location

State the location of the sampling or experiment, providing relevant parameters (e.g. latitude and longitude, elevation, water depth).

Access & import/export

Describe the efforts you have made to access habitats and to collect and import/export your samples in a responsible manner and in compliance with local, national and international laws, noting any permits that were obtained (give the name of the issuing authority, the date of issue, and any identifying information).

Disturbance

Describe any disturbance caused by the study and how it was minimized.

Reporting for specific materials, systems and methods

We require information from	authors	about some types of materials, experimental systems and methods used in many studies. Here, indicate whether each material,			
		your study. If you are not sure if a list item applies to your research, read the appropriate section before selecting a response.			
Materials & experime n/a Involved in the study Antibodies Eukaryotic cell lines Palaeontology and Animals and other of the color of	s archaeo organism articipan	n/a Involved in the study ChIP-seq Flow cytometry MRI-based neuroimaging Involved in the study ChIP-seq MRI-based neuroimaging Involved in the study ChIP-seq Flow cytometry Involved in the study ChIP-seq Flow cytometry Involved in the study Involved in the study ChIP-seq Flow cytometry Involved in the study Involved in the study ChIP-seq Involved in the study ChIP-seq Involved in the study ChIP-seq Involved in the study Involved in the			
Antibodies used	Descri	be all antibodies used in the study; as applicable, provide supplier name, catalog number, clone name, and lot number.			
Validation Describe the validation of each primary antibody for the species and application, noting any validation statements on the manufacturer's website, relevant citations, antibody profiles in online databases, or data provided in the manuscript.					
Eukaryotic cell lir	ies				
Policy information about <u>c</u>	<u>ell lines</u>				
Cell line source(s)		State the source of each cell line used.			
Authentication		Describe the authentication procedures for each cell line used OR declare that none of the cell lines used were authenticated.			
Mycoplasma contaminat	ion	Confirm that all cell lines tested negative for mycoplasma contamination OR describe the results of the testing for mycoplasma contamination OR declare that the cell lines were not tested for mycoplasma contamination.			
Commonly misidentified (See ICLAC register)	lines	Name any commonly misidentified cell lines used in the study and provide a rationale for their use.			
Palaeontology an	d Ar	chaeology			
Specimen provenance					
Specimen deposition	Indicate where the specimens have been deposited to permit free access by other researchers.				
Dating methods	If new dates are provided, describe how they were obtained (e.g. collection, storage, sample pretreatment and measurement), when they were obtained (i.e. lab name), the calibration program and the protocol for quality assurance OR state that no new dates are provided.				
Tick this box to confi	m that	the raw and calibrated dates are available in the paper or in Supplementary Information.			
Ethics oversight	thics oversight Identify the organization(s) that approved or provided guidance on the study protocol, OR state that no ethical approval or guidance was required and explain why not.				
Note that full information on	the appr	oval of the study protocol must also be provided in the manuscript.			

Animals and other organisms

Policy information about studies involving animals; ARRIVE guidelines recommended for reporting animal research

Laboratory animals

For laboratory animals, report species, strain, sex and age OR state that the study did not involve laboratory animals.

Wild animals

Provide details on animals observed in or captured in the field; report species, sex and age where possible. Describe how animals were caught and transported and what happened to captive animals after the study (if killed, explain why and describe method; if released, say where and when) OR state that the study did not involve wild animals.

Field-collected samples

For laboratory work with field-collected samples, describe all relevant parameters such as housing, maintenance, temperature, photoperiod and end-of-experiment protocol OR state that the study did not involve samples collected from the field.

Ethics oversight

Identify the organization(s) that approved or provided guidance on the study protocol, OR state that no ethical approval or guidance was required and explain why not.

Note that full information on the approval of the study protocol must also be provided in the manuscript.

Human research participants

Dolic	v information	about ct	tudiac invo	lving	human	recearch	narticinants
POIIC	v imormation	about Si	Luaies irivo	iving.	numan	research	participants

Population characteristics

Describe the covariate-relevant population characteristics of the human research participants (e.g. age, gender, genotypic information, past and current diagnosis and treatment categories). If you filled out the behavioural & social sciences study design questions and have nothing to add here, write "See above."

Recruitment

Describe how participants were recruited. Outline any potential self-selection bias or other biases that may be present and how these are likely to impact results.

Ethics oversight

Identify the organization(s) that approved the study protocol.

Note that full information on the approval of the study protocol must also be provided in the manuscript.

Clinical data

Policy information about clinical studies

All manuscripts should comply with the ICMJE guidelines for publication of clinical research and a completed CONSORT checklist must be included with all submissions.

Clinical trial registration

Provide the trial registration number from ClinicalTrials.gov or an equivalent agency.

Study protocol

Note where the full trial protocol can be accessed OR if not available, explain why.

Describe the settings and locales of data collection, noting the time periods of recruitment and data collection.

Outcomes

Describe how you pre-defined primary and secondary outcome measures and how you assessed these measures.

Dual use research of concern

Policy information about <u>dual use research of concern</u>

Hazards

Could the accidental, deliberate or reckless misuse of agents or technologies generated in the work, or the application of information presented in the manuscript, pose a threat to:

No	Yes
	Public health
	National security
	Crops and/or livestock
	Ecosystems
	Any other significant area

Experiments of concern

Does the work involve any of these experiments of concern:

No	Yes
	Demonstrate how to render a vaccine ineffective
	Confer resistance to therapeutically useful antibiotics or antiviral agents
	Enhance the virulence of a pathogen or render a nonpathogen virulent
	Increase transmissibility of a pathogen
	Alter the host range of a pathogen
	Enable evasion of diagnostic/detection modalities
	Enable the weaponization of a biological agent or toxin
	Any other potentially harmful combination of experiments and agents

	_ 1		_	_	_
	n	ייו	-c	0	П
\sim			J	$\overline{}$	ч

Data deposition

Confirm that both raw and final processed data have been deposited in a public database such as GEO.

Confirm that you have deposited or provided access to graph files (e.g. BED files) for the called peaks.

Data access links

May remain private before publication.

For "Initial submission" or "Revised version" documents, provide reviewer access links. For your "Final submission" document, provide a link to the deposited data.

Files in database submission

Provide a list of all files available in the database submission.

Genome browser session (e.g. UCSC)

Provide a link to an anonymized genome browser session for "Initial submission" and "Revised version" documents only, to enable peer review. Write "no longer applicable" for "Final submission" documents.

Methodology

Replicates Describe the experimental replicates, specifying number, type and replicate agreement.

Sequencing depth Describe the sequencing depth for each experiment, providing the total number of reads, uniquely mapped reads, length of reads and whether they were paired- or single-end.

Describe the antibodies used for the ChIP-seq experiments; as applicable, provide supplier name, catalog number, clone name, and lot **Antibodies**

Peak calling parameters

Specify the command line program and parameters used for read mapping and peak calling, including the ChIP, control and index files

Describe the methods used to ensure data quality in full detail, including how many peaks are at FDR 5% and above 5-fold enrichment.

Software

Data quality

Describe the software used to collect and analyze the ChIP-seq data. For custom code that has been deposited into a community repository, provide accession details

Flow Cytometry

Plots

Confirm that:

The axis labels state the marker and fluorochrome used (e.g. CD4-FITC).

The axis scales are clearly visible. Include numbers along axes only for bottom left plot of group (a 'group' is an analysis of identical markers).

All plots are contour plots with outliers or pseudocolor plots.

A numerical value for number of cells or percentage (with statistics) is provided.

Methodology

Sample preparation Describe the sample preparation, detailing the biological source of the cells and any tissue processing steps used.

Instrument Identify the instrument used for data collection, specifying make and model number.

Software Describe the software used to collect and analyze the flow cytometry data. For custom code that has been deposited into a

community repository, provide accession details.

Describe the abundance of the relevant cell populations within post-sort fractions, providing details on the purity of the Cell population abundance

samples and how it was determined.

Describe the gating strategy used for all relevant experiments, specifying the preliminary FSC/SSC gates of the starting cell Gating strategy

population, indicating where boundaries between "positive" and "negative" staining cell populations are defined.

Tick this box to confirm that a figure exemplifying the gating strategy is provided in the Supplementary Information.

Magnetic resonance imaging

Experimental design

Design type

Indicate task or resting state; event-related or block design.

0 1		e number of blocks, trials or experimental units per session and/or subject, and specify the length of each trial ftrials are blocked) and interval between trials.
Behavioral performance measur		ber and/or type of variables recorded (e.g. correct button press, response time) and what statistics were used h that the subjects were performing the task as expected (e.g. mean, range, and/or standard deviation across
Acquisition		
Imaging type(s)	Specify: fu	nctional, structural, diffusion, perfusion.
Field strength	Specify in	Tesla
Sequence & imaging parameters		e pulse sequence type (gradient echo, spin echo, etc.), imaging type (EPI, spiral, etc.), field of view, matrix size, ness, orientation and TE/TR/flip angle.
Area of acquisition	State whe	ther a whole brain scan was used OR define the area of acquisition, describing how the region was determined.
Diffusion MRI Used	☐ Not u	sed
Preprocessing		
Preprocessing software		n software version and revision number and on specific parameters (model/functions, brain extraction, smoothing kernel size, etc.).
Normalization		rmalized/standardized, describe the approach(es): specify linear or non-linear and define image types used for OR indicate that data were not normalized and explain rationale for lack of normalization.
Normalization template		mplate used for normalization/transformation, specifying subject space or group standardized space (e.g. ch, MNI305, ICBM152) OR indicate that the data were not normalized.
Noise and artifact removal		rocedure(s) for artifact and structured noise removal, specifying motion parameters, tissue signals and gnals (heart rate, respiration).
Volume censoring	Define your sof	tware and/or method and criteria for volume censoring, and state the extent of such censoring.
Statistical modeling & infere	nce	
Model type and settings		ass univariate, multivariate, RSA, predictive, etc.) and describe essential details of the model at the first and .g. fixed, random or mixed effects; drift or auto-correlation).
Effect(s) tested		effect in terms of the task or stimulus conditions instead of psychological concepts and indicate whether orial designs were used.
Specify type of analysis: W	hole brain [ROI-based Both
Statistic type for inference (See <u>Eklund et al. 2016</u>)	Specify voxel-w	ise or cluster-wise and report all relevant parameters for cluster-wise methods.
Correction	Describe the ty	pe of correction and how it is obtained for multiple comparisons (e.g. FWE, FDR, permutation or Monte Carlo).
Models & analysis		
n/a Involved in the study Functional and/or effective Graph analysis Multivariate modeling or p		s
Functional and/or effective connectivity		Report the measures of dependence used and the model details (e.g. Pearson correlation, partial correlation, mutual information).
Graph analysis		Report the dependent variable and connectivity measure, specifying weighted graph or binarized graph, subject- or group-level, and the global and/or node summaries used (e.g. clustering coefficient, efficiency, etc.).
Multivariate modeling and predictive analysis		Specify independent variables, features extraction and dimension reduction, model, training and evaluation metrics.